Steels for Hydrogen Service at Elevated Temperatures and Pressures in Petroleum Refineries and Petrochemical Plants

API RECOMMENDED PRACTICE 941
EIGHTH EDITION, FEBRUARY 2016

ERRATA 1, JUNE 2016
ERRATA 2, JANUARY 2018

ADDENDUM 1, AUGUST 2020

Special Notes

API publications necessarily address problems of a general nature. With respect to particular circumstances, local, state, and federal laws and regulations should be reviewed. The use of API publications is voluntary. In some cases, third parties or authorities having jurisdiction may choose to incorporate API standards by reference and may mandate compliance.

Neither API nor any of API's employees, subcontractors, consultants, committees, or other assignees make any warranty or representation, either express or implied, with respect to the accuracy, completeness, or usefulness of the information contained herein, or assume any liability or responsibility for any use, or the results of such use, of any information or process disclosed in this publication. Neither API nor any of API's employees, subcontractors, consultants, or other assignees represent that use of this publication would not infringe upon privately owned rights.

API publications may be used by anyone desiring to do so. Every effort has been made by the Institute to assure the accuracy and reliability of the data contained in them; however, the Institute makes no representation, warranty, or guarantee in connection with this publication and hereby expressly disclaims any liability or responsibility for loss or damage resulting from its use or for the violation of any authorities having jurisdiction with which this publication may conflict.

API publications are published to facilitate the broad availability of proven, sound engineering and operating practices. These publications are not intended to obviate the need for applying sound engineering judgment regarding when and where these publications should be utilized. The formulation and publication of API publications is not intended in any way to inhibit anyone from using any other practices.

Any manufacturer marking equipment or materials in conformance with the marking requirements of an API standard is solely responsible for complying with all the applicable requirements of that standard. API does not represent, warrant, or guarantee that such products do in fact conform to the applicable API standard.

Classified areas may vary depending on the location, conditions, equipment, and substances involved in any given situation. Users of this Recommended Practice should consult with the appropriate authorities having jurisdiction.

Users of this Recommended Practice should not rely exclusively on the information contained in this document. Sound business, scientific, engineering, and safety judgment should be used in employing the information contained herein.

API is not undertaking to meet the duties of employers, manufacturers, or suppliers to warn and properly train and equip their employees, and others exposed, concerning health and safety risks and precautions, nor undertaking their obligations to comply with authorities having jurisdiction.

Information concerning safety and health risks and proper precautions with respect to particular materials and conditions should be obtained from the employer, the manufacturer or supplier of that material, or the material safety data sheet.

Where applicable, authorities having jurisdiction should be consulted.

Work sites and equipment operations may differ. Users are solely responsible for assessing their specific equipment and premises in determining the appropriateness of applying the Recommended Practice. At all times users should employ sound business, scientific, engineering, and judgment safety when using this Recommended Practice.

Foreword

Nothing contained in any API publication is to be construed as granting any right, by implication or otherwise, for the manufacture, sale, or use of any method, apparatus, or product covered by letters patent. Neither should anything contained in the publication be construed as insuring anyone against liability for infringement of letters patent.

Shall: As used in a standard, “shall” denotes a minimum requirement in order to conform to the specification.

Should: As used in a standard, “should” denotes a recommendation or that which is advised but not required in order to conform to the specification.

May: As used in a standard, "may" denotes a course of action permissible within the limits of a standard.

Can: As used in a standard, "can" denotes a statement of possibility or capability.

This document was produced under API standardization procedures that ensure appropriate notification and participation in the developmental process and is designated as an API standard. Questions concerning the interpretation of the content of this publication or comments and questions concerning the procedures under which this publication was developed should be directed in writing to the Director of Standards, American Petroleum Institute, 200 Massachusetts Avenue, NW, Suite 1100, Washington, DC 20001. Requests for permission to reproduce or translate all or any part of the material published herein should also be addressed to the director.

Generally, API standards are reviewed and revised, reaffirmed, or withdrawn at least every five years. A one-time extension of up to two years may be added to this review cycle. Status of the publication can be ascertained from the API Standards Department, telephone (202) 682-8000. A catalog of API publications and materials is published annually by API, 200 Massachusetts Avenue, NW, Suite 1100, Washington, DC 20001.

Suggested revisions are invited and should be submitted to the Standards Department, API, 200 Massachusetts Avenue, NW, Suite 1100, Washington, DC 20001, standards@api.org.

Contents

Figures

Contents

Tables

Introduction

At normal atmospheric temperatures, gaseous molecular hydrogen does not readily permeate steel, even at high pressures. Carbon steel is the standard material for cylinders that are used to transport hydrogen at pressures of 2000 psi (14 MPa). Many postweld heat treated carbon steel pressure vessels have been used successfully in continuous service at pressures up to 10,000 psi (69 MPa) and temperatures up to 430 °F (221 °C). However, under these same conditions, highly stressed carbon steels and hardened steels have cracked due to hydrogen embrittlement.

The recommended maximum hydrogen partial pressure at atmospheric temperature for carbon steel fabricated in accordance with the ASME *Boiler and Pressure Vessel Code* is 13,000 psia (90 MPa). Below this pressure, carbon steel equipment has shown satisfactory performance. Above this pressure, very little operating and experimental data are available. If plants are to operate at hydrogen partial pressures that exceed 13,000 psia (90 MPa), the use of an austenitic stainless steel liner with venting in the shell should be considered.

At elevated temperatures, molecular hydrogen dissociates into the atomic form, which can readily enter and diffuse through the steel. Under these conditions, the diffusion of hydrogen in steel is more rapid. As discussed in Section 4, hydrogen reacts with the carbon in the steel to cause either surface decarburization or internal decarburization and fissuring, and eventual cracking. This form of hydrogen damage is called high temperature hydrogen attack (HTHA), and this recommended practice discusses the resistance of steels to HTHA.

Steels for Hydrogen Service at Elevated Temperatures and Pressures in Petroleum Refineries and Petrochemical Plants

1 Scope

This recommended practice (RP) summarizes the results of experimental tests and actual data acquired from operating plants to establish practical operating limits for carbon and low alloy steels in hydrogen service at elevated temperatures and pressures. The effects on the resistance of steels to hydrogen at elevated temperature and pressure that result from high stress, heat treatment, chemical composition, and cladding are discussed. This RP does not address the resistance of steels to hydrogen at lower temperatures [below about 400 °F (204 °C)], where atomic hydrogen enters the steel as a result of an electrochemical mechanism.

This RP applies to equipment in refineries, petrochemical facilities, and chemical facilities in which hydrogen or hydrogen-containing fluids are processed at elevated temperature and pressure. The guidelines in this RP can also be applied to hydrogenation plants such as those that manufacture ammonia, methanol, edible oils, and higher alcohols.

The steels discussed in this RP resist high temperature hydrogen attack (HTHA) when operated within the guidelines given. However, they may not be resistant to other corrosives present in a process stream or to other metallurgical damage mechanisms that can occur in the operating HTHA range. This RP also does not address the issues surrounding possible damage from rapid cooling of the metal after it has been in high temperature, high pressure hydrogen service (e.g. possible need for outgassing hydroprocessing reactors). This RP discusses in detail only the resistance of steels to HTHA.

Presented in this document are curves that indicate the operating limits of temperature and hydrogen partial pressure for satisfactory resistance of carbon steel and Cr-Mo steels to HTHA in elevated temperature hydrogen service. In addition, it includes a summary of inspection methods to evaluate equipment for the existence of HTHA.

2 Normative References

The following documents are referred to in the text in such a way that some or all of their content constitutes requirements of this document. For undated references, the latest edition of the referenced document (including any addenda) applies.

API 510, *Pressure Vessel Inspection Code: In-Service Inspection, Rating, Repair, and Alteration*

API 570, *Piping Inspection Code: In-Service Inspection, Rating, Repair, and Alteration of Piping Systems*

API Recommended Practice 584, *Integrity Operating Windows*

ASME *Boiler and Pressure Vessel Code* (*BPVC*) [1], *Section VIII: Pressure Vessels; Division 1*

ASME *Boiler and Pressure Vessel Code* (*BPVC*), *Section VIII: Pressure Vessels; Division 2*

ASME/ANSI [2] *Code for Pressure Piping* B31.3, *Chemical Plant and Petroleum Refinery Piping*

AWS D10.10/D10.10M [3], *Recommended Practices for Local Heating of Welds in Piping and Tubing*

WRC Bul-452 [4], *Recommended Practices for Local Heating of Welds in Pressure Vessels*

[1] ASME International, 2 Park Avenue, New York, New York 10016-5990, www.asme.org.
[2] American National Standards Institute, 25 West 43rd Street, 4th Floor, New York, New York 10036, www.ansi.org.
[3] American Welding Society, 8669 NW 36 Street, # 130, Miami, Florida 33166-6672, www.aws.org
[4] Welding Research Council, P.O. Box 201547, Shaker Heights, Ohio 44122, www.forengineers.org

3 Operating Experience

3.1 Basis for Setting Integrity Operating Windows

Figure 1 illustrates the resistance of steels to attack by hydrogen at elevated temperatures and hydrogen pressures. HTHA of steel can result in surface decarburization, internal decarburization, fissuring, and cracking, or a combination of these (see Section 4). Figure 1 gives the operating conditions (process temperature and hydrogen partial pressure) above which these types of damage can occur.

Figure 1 is based upon experience gathered since the 1940s. Supporting data were obtained from a variety of commercial processes and laboratory experiments (see the References to Figure 1). While temperature and hydrogen partial pressure data were not always known precisely, the accuracy is often sufficient for commercial use. Satisfactory performance has been plotted only for samples or equipment exposed for at least 1 year. Unsatisfactory performance from laboratory or plant data has been plotted, regardless of the length of exposure time. The chemical compositions of the steels in Figure 1 should conform to the limits specified for the various grades by ASTM/ASME.

Owners/operators should develop integrity operating windows (IOWs) (as outlined in API 584) to manage risks associated with HTHA by using operational experience presented in this document.

Since the original version of Figure 1 was prepared for API in 1949 [1], further experience has enabled curves for most commonly used steels to be more accurately located. All information relevant to 0.5Mo steels (C-0.5Mo and Mn-0.5Mo) is summarized in Annex A.

The Fifth Edition of this RP also added three data points, which show HTHA of 1.25Cr-0.5Mo steel below the current 1.25Cr-0.5Mo curve. See Annex B for more discussion of 1.25Cr-0.5Mo steel. Annex C gives a similar discussion for 2.25Cr-1.0Mo steel.

This Eighth Edition adds 12 data points and a new curve labeled as “Carbon steel (welded with no PWHT)” for HTHA of carbon steel not subjected to postweld heat treatment (PWHT), which is below the carbon steel curve appearing in all previous editions and now labeled as “Carbon steel (non-welded or welded with PWHT).” See Annex F for more discussion on carbon steel welds not subjected to PWHT.

3.2 Selecting Materials for New Equipment

The API Subcommittee on Corrosion and Materials collects data on the alloys shown in all figures or similar alloys that may come into use. Follow the guidance in Annex H for submitting new data.

Figure 1 is often used when selecting materials for new equipment in hydrogen service. When using Figure 1 as an aid for materials selection, it is important to recognize that Figure 1 only addresses a material’s resistance to HTHA. It does not take into account other factors important at high temperatures such as:

a) other corrosive species that may be in the system such as hydrogen sulfide;

b) creep, temper embrittlement, or other high temperature damage mechanisms;

c) interaction of hydrogen and stress (primary, secondary, and residual); and

d) synergistic effects such as between HTHA and creep.

Temperatures for data plotted in the figures represent a range in operating conditions that in previous editions was stated to be about ±20 °F (±11 °C). Because of the uncertainty of the actual operating conditions over many decades of operation for data points contained in the curves, users need to understand that Figure 1 is based largely upon empirical experience and from the guidance in API TR 941 [39]. Therefore, an operating company should add a safety margin, below the relevant curve, when selecting steels.

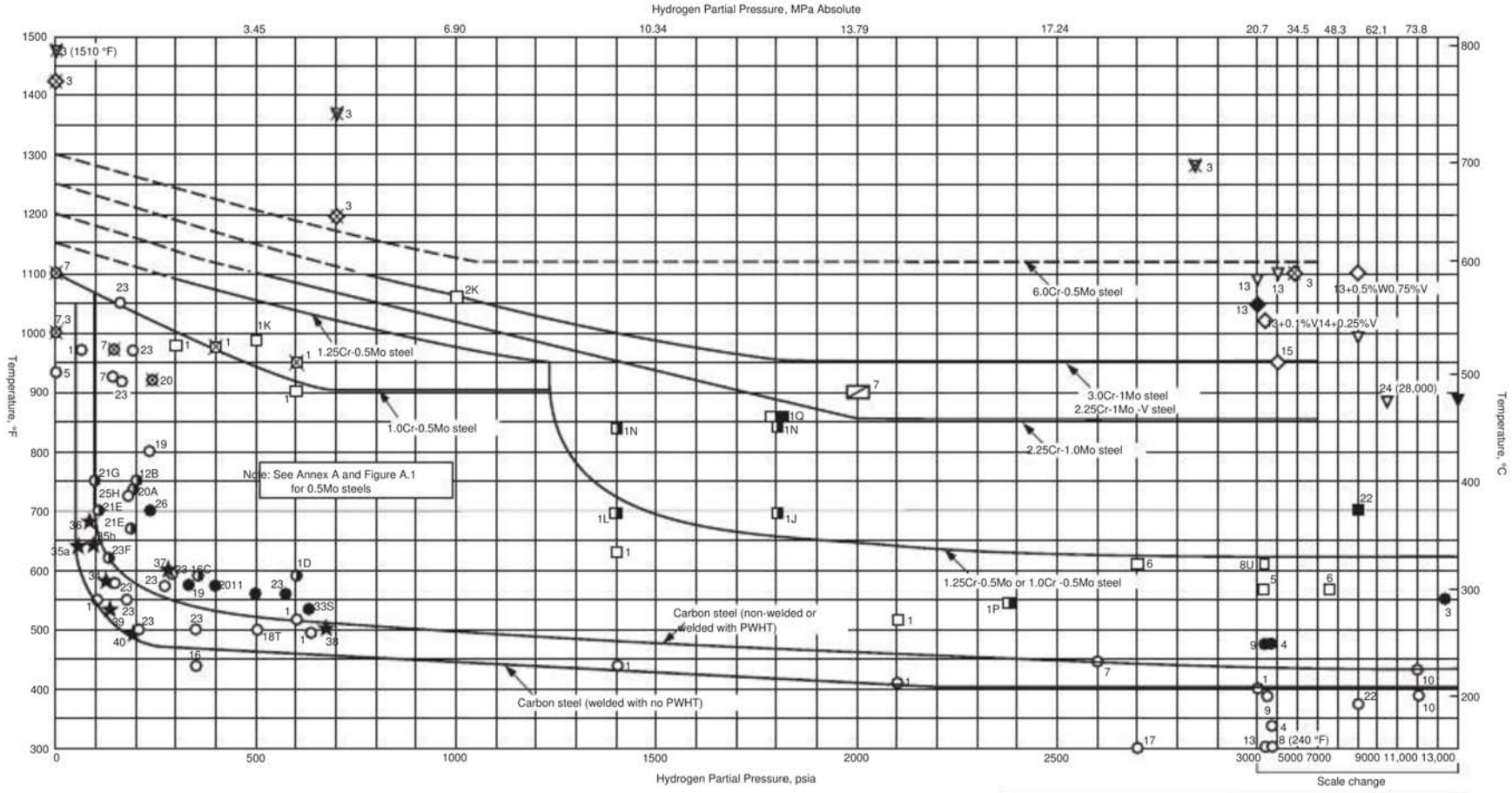

The limits described by these curves are based on service experience originally collected by G.A. Nelson and on additional information gathered by or made available to API.

NOTE 2 Austenitic stainless steels are generally not decarburized in hydrogen at any temperature or hydrogen pressure.

NOTE 3 The limits described by these curves are based on experience with cast steel as well as annealed and normalized steels at stress levels defined by Section VIII, Division 1, of the ASME Code. See 5.3 and 5.4 in text for additional information.

NOTE 4 Several failures of 1.25Cr 1-Mo steel have been reported in the satisfactory region. See Annex B for details.

NOTE 5 The inclusion of the 2.25Cr-1Mo-V class of steels is based on 10,000+hr laboratory tests where these alloys were at least equal to the 3Cr-1Mo steel. See Reference [22] listed in the Bibliography.

This figure was revised by API in 1969, 1983, 1990, 1996, and 2015.

Figure 1—Operating Limits for Steels in Hydrogen Service to Avoid High Temperature Hydrogen Attack

3.3 High Temperature Hydrogen Attack (HTHA) in a Liquid Hydrocarbon Phase

HTHA can occur in a liquid hydrocarbon phase if it can occur in the gas phase in equilibrium with the liquid phase. For materials selection purposes (using Figure 1), hydrogen dissolved in liquid hydrocarbon should be assumed to exert a vapor pressure equal to the hydrogen partial pressure of the gas with which the liquid is, or was last, in equilibrium. Recent plant experience and testing of field-exposed specimens have shown that HTHA can occur under such conditions [10].

HTHA has been found in liquid-filled carbon steel piping downstream of a heavy oil desulfurization unit separator that was operating at hydrogen partial pressure and temperature conditions above the Figure 1 welded with PWHT carbon steel curve. Testing of field-exposed test specimens showed HTHA of both chrome-plated and bare carbon steel samples that were totally immersed in liquid [10].

Several HTHA failures were found in liquid-filled carbon steel piping not subject to PWHT downstream of gasoline desulfurization unit reactors that were operating at hydrogen partial pressures and temperatures below the welded and PWHT carbon steel curve as it appeared in Figure 1 in previous editions of this RP. See Annex F for more discussion of non-PWHT'd carbon steel. See Annex G for more discussion on how to calculate the hydrogen partial pressure in liquid-filled equipment and piping.

3.4 Base Material for Refractory-lined Equipment or Piping

For cold-wall refractory-lined equipment or piping, there can be a risk of HTHA when:

— the internal process conditions are above the relevant carbon steel curve of Figure 1, and

— the refractory becomes degraded or there is gas bypass behind the refractory, resulting in a hot spot on the outer shell.

The materials selection for the outer shell should consider the risk and possible severity of metal hot spots due to refractory damage. The risk of hot spots is greater if the refractory is known to experience erosion or other degradation mechanisms in the specific service. The risk level may be mitigated if there are effective techniques of promptly detecting hot spots and efficient means of keeping the hot spot areas cooled. As such, owners/operators should inspect refractory-lined equipment periodically with thermography and mitigate the hot spots with air/steam to a temperature below the Nelson curve, but above any process dew point.

A more reliable way of protecting the base metal in refractory-lined equipment with a risk of HTHA is to select materials resistant to the internal hydrogen partial pressure and predicted hot spot temperatures. The design can still take advantage of higher allowable stresses at the cooler refractory-protected temperatures to enable less wall thickness, while protecting the base metal from the potential of HTHA failure.

3.5 References and Comments for Figure 1

NOTE The data points in Figure 1 are labeled with reference numbers corresponding to the sources listed in 3.5.1. The letters in the figure correspond to the comments listed in 3.5.2.

3.5.1 Figure 1 References

1) Shell Oil Company, private communication to API Subcommittee on Corrosion.

2) Timken Roller Bearing Company, private communication to API Subcommittee on Corrosion.

3) F.K. Naumann, "Influence of Alloy Additions to Steel Upon Resistance to Hydrogen Under High Pressure," *Technische Mitieilungen Krupp*, Vol. 1, No. 12, pp. 223–234, 1938.

4) N.P. Inglis and W. Andrews, “The Effect on Various Steels of Hydrogen at High Pressure and Temperature,” *Journal of the Iron and Steel Institute*, Vol. 128, No. 2, pp. 383–397, 1933.

5) J.L. Cox, “What Steel to Use at High Pressures and Temperatures,” *Chemical and Metallurgical Engineering*, Vol. 40, pp. 405–409, 1933.

6) R.J. Sargant and T.H. Middleham, “Steels for Autoclaves,” *Chemical Engineering Congress Transactions*, Vol. I, World Power Conference, London, pp. 66–110, June 1936.

7) Standard Oil Company of California, private communication to API Subcommittee on Corrosion.

8) E.I. du Pont de Nemours and Company, private communication to API Subcommittee on Corrosion.

9) Ammoniawerk Merseberg, private communication to API Subcommittee on Corrosion, 1938.

10) Hercules Powder Company, private communication to API Subcommittee on Corrosion.

11) C.A. Zapffe, “Boiler Embrittlement,” *Transactions of the ASME*, Vol. 66, pp. 81–126, 1944.

12) The M.W. Kellogg Company, private communication to API Subcommittee on Corrosion.

13) German operating experience, private communication to API Subcommittee on Corrosion, 1946.

14) Vanadium Corporation of America, private communication to API Subcommittee on Corrosion.

15) Imperial Chemical Industries, Billingham, England, private communication to API Subcommittee on Corrosion.

16) T.C. Evans, “Hydrogen Attack on Carbon Steels,” *Mechanical Engineering*, Vol. 70, pp. 414–416, 1948.

17) Norweg Hydroelectric, Oslo, Norway, private communication to API Subcommittee on Corrosion.

18) Union Oil Company of California, private communication to API Subcommittee on Corrosion, 1980.

19) A.R. Ciuffreda and W.D. Rowland, “Hydrogen Attack of Steel in Reformer Service,” *Proceedings*, Vol. 37, API, New York, pp. 116–128, 1957.

20) API Refinery Corrosion Committee Survey, 1957.

21) Air Products, Inc., private communication to API Subcommittee on Corrosion, March 1960.

22) G.D. Gardner and J.T. Donovan, “Corrosion and Erosion in the Synthetic Fuels Demonstration Plants,” *Transactions of the ASME*, Vol. 75, pp. 525–533, 1953.

23) Amoco Oil Company, private communication to API Subcommittee on Corrosion, 1960.

24) E.W. Comings, *High Pressure Technology*, McGraw-Hill, New York, 1956.

25) M. Hasegawa and S. Fujinaga, “Attack of Hydrogen on Oil Refinery Steels,” *Tetsu To Hagane*, Vol. 46, No. 10, pp. 1349–1352, 1960.

26) K.L. Moore and D.B. Bird, “How to Reduce Hydrogen Plant Corrosion,” *Hydrocarbon Processing*, Vol. 44, No. 5, pp. 179–184, 1965.

27) Union Oil Company of California, private communication to API Subcommittee on Corrosion, 1976.

28) Amoco Oil Company, private communication to API Subcommittee on Corrosion, 1976.

29) Standard Oil Company of California, private communication to API Subcommittee on Corrosion, 1976.

30) Exxon Corporation, private communication to API Subcommittee on Corrosion, 1976.

31) Shell Oil Company, private communication to API Subcommittee on Corrosion, 1976.

32) Cities Service Company, private communication to API Subcommittee on Corrosion, 1976.

33) Gulf Oil Corporation, private communication to API Subcommittee on Corrosion, 1976.

34) J. McLaughlin, J. Krynicki, and T. Bruno, "Cracking of non-PWHT'd Carbon Steel Operating at Conditions Immediately Below the Nelson Curve," *Proceedings of 2010 ASME Pressure Vessels and Piping Conference, July 2010, Bellevue Washington*, PVP2010-25455.

35) Eight separate points 35a through 35h. Valero Energy Corporation, private communication to API Subcommittee on Corrosion, 2012.

36) Phillips 66 Company, private communication to API Subcommittee on Corrosion, 2012.

37) Phillips 66 Company, private communication to API Subcommittee on Corrosion, 2012.

38) Total Refining and Marketing, private communication to API Subcommittee, 2011.

39) Marathon Petroleum Co., private communication to API Subcommittee, 2014.

40) Marathon Petroleum Co., private communication to API Subcommittee, 2014.

3.5.2 Figure 1 Comments

A) A section made of A106 pipe was found to be damaged to 27 % of its thickness after 5745 hours. Other pieces of pipe in the same line were unaffected.

B) The damage was concentrated in the overheated section of a hot bent steel elbow. The unheated straight portions of the elbow were not attacked.

C) In a series of 29 steel samples, 12 were damaged, while 17 were not.

D) After 2 years exposure, five out of six pieces of carbon steel pipe were damaged. One piece of pipe was unaffected.

E) Damage was concentrated in the weld and heat-affected sections of A106 pipe. Base metal on either side of this zone was unaffected.

F) After 11 years of service, damage was found in the hot bent section of A106 pipe. Unheated straight sections were not affected.

G) After 2 years of service, all parts of carbon steel pipe, including weld and heat-affected zone (HAZs), were satisfactory.

H) After 4 years of service, weld and HAZs of A106 pipe showed cracks.

J) After 31 years of service, a forging of 0.3C-1.3Cr-0.25Mo steel showed cracks 0.007 in. (0.2 mm) deep.

K) Pipes of 1.25Cr-0.25Mo steel.

L) After 4 years of service, a forging of 0.3C-1.3Cr-0.25Mo steel was unaffected.

N) After 7 years of service, a forging of 0.3C-1.52Cr-0.50Mo steel showed cracks 0.050 in. (1.3 mm) deep.

P) After 30 years of service, a forging of 0.30C-0.74Cr-0.43Ni steel was unaffected.

Q) After 15 years in ammonia service, a pipe of 0.15C-2.25Cr-1.00Mo steel showed no HTHA but was nitrided to a depth of 0.012 in. (0.3 mm).

S) After 8 years, carbon steel cracked.

T) After 18 years, carbon steel did not show HTHA.

U) After 450 days exposure, a 1.25Cr-0.5Mo valve body was not damaged by HTHA.

V) Point 34. After 30+ years non-PWHT'd carbon steel reactor, vessels, and associated piping in light distillate hydrotreating service cracked from HTHA. Operating at roughly 580 °F (304 °C) and at 125 psia (0.86 MPa).

W) Points 35a and 35h. These 2 points on the plot represent the range of 8 different failures. After 4.5 to 8 years, 7 different non-PWHT'd carbon steel flanges cracked in the HAZs on the flange side of a flange-to-pipe weld in gasoline hydrotreating service. One cracked on the pipe side of the pipe-to-flange weld. Operating at roughly 645 °F (340 °C) and at 57 psia to 94 psia (0.39 MPa to 0.65 MPa) hydrogen partial pressure.

X) Point 37. After 14 years, a non-PWHT'd SA-105 carbon steel flange cracked in the HAZ on the flange side of a flange-to-pipe weld. Operating at roughly 600 °F (316 °C) and at 280 psia (1.9 MPa).

Y) Point 36. After 6 years, multiple non-PWHT'd carbon steel flanges cracked in the HAZs on the flange side of a flange to pipe welds in a gasoline desulfurization unit. Operating at roughly 670 °F (354 °C) and at 85 psia (0.59 MPa).

Z) Point 38. After 29 years, a non-PWHT'd carbon steel exchanger shell in Hydrodesulfurization (HDS) service cracked. Operating at roughly 500 °F (260 °C) and at 670 psia (4.6 MPa).

A.1) Point 39. After 10 years, inspection found cracks in a non-PWHT'd carbon steel exchanger shell in light hydrotreater service. Operating at roughly 540°F (282 °C) and at 130 psia (0.90 MPa).

B.1) Point 40. After 30+ years, inspection found cracks in a non-PWHT'd carbon steel exchanger shell in light hydrotreater service. Operating at roughly 490 °F (254 °C) and at 195 psia (1.3 MPa).

4 Forms of HTHA

4.1 General

High temperature hydrogen can attack steels in two ways:

a) surface decarburization, and

b) internal decarburization and fissuring, eventually leading to cracking.

The combination of high temperature and low hydrogen partial pressure favors surface decarburization without internal decarburization and fissuring. The combination of low temperature, but above 400 °F (204 °C), and high hydrogen partial pressure, above 2200 psia (15.17 MPa), favors internal decarburization and fissuring, which can eventually lead to cracking. At high temperatures and high hydrogen partial pressures, both mechanisms are active. These mechanisms are described in detail below.

The broken-line curves at the top of Figure 1 represent the tendencies for surface decarburization of steels while they are in contact with hydrogen. The solid-line curves represent the tendencies for steels to decarburize internally with resultant fissuring and cracking.

4.2 Surface Decarburization

Surface decarburization without fissuring has been associated with hydrogen partial pressure and temperature conditions that are not severe enough to generate the methane pressures needed to form fissures. This typically occurs in carbon steel where the Nelson curves become vertical [39].

Surface decarburization as a form of HTHA is similar to that resulting from the high-temperature exposure of steel to certain other gases such as air, oxygen, or carbon dioxide. The usual effects of surface decarburization are a slight, localized reduction in strength and hardness and an increase in ductility. Because these effects are usually small, there is often much less concern with surface decarburization than there is with internal decarburization.

A number of theories have been proposed to explain surface decarburization [2] [3] [4], but the currently accepted view is based on the migration of carbon to the surface where gaseous compounds of carbon are formed, rendering the steel less rich in carbon. The gaseous compounds formed are CH_4 or, when oxygen-containing gases are present, CO. Water vapor hastens the reaction. While carbon in solution diffuses to the surface to form gaseous carbon compounds, the carbon in solution is continuously supplied from the carbide compounds in the steel. Thus, carbide stability is directly related to the rate of surface decarburization.

In cases where surface decarburization predominates over internal attack, the actual values of pressure-temperature combinations have not been extensively studied, but the limits defined by Naumann [5] probably give the most accurate trends.

4.3 Internal Decarburization, Fissuring, and Cracking

The solid-line curves in Figure 1 define the areas above which material damage by internal decarburization and fissuring/cracking have been reported. Below and to the left of the curve for each alloy, satisfactory performance has been experienced with periods of exposure of up to approximately 60 years. At temperatures above and to the right of the solid curves, there is a probability that internal decarburization and fissuring/cracking may occur. Internal decarburization and fissuring are preceded by a period of time where no immediate damage is detected, and this is often referred to as an “incubation period.” The incubation period depends on temperature and hydrogen partial pressure (see 5.1 for further discussion).

Internal decarburization and fissuring are caused by hydrogen permeating the steel and reacting with carbon to form methane [5]. The methane formed cannot diffuse out of the steel and typically accumulates at grain boundaries. This results in high localized stresses that lead to the formation of fissures, cracks, or blisters in the steel. Fissures in hydrogen-damaged steel lead to a substantial deterioration of mechanical properties.

Figure 2 shows the microstructure of a sample of C-0.5Mo steel damaged by internal decarburization and fissuring. The service conditions were 790 °F (421 °C) at a hydrogen partial pressure of 425 psia (2.9 MPa) for approximately 65,000 hours in a catalytic reformer.

The addition of carbide stabilizers to steel reduces the tendency toward internal fissuring. Elements, such as chromium, molybdenum, tungsten, vanadium, titanium, and niobium, form more stable alloy carbides that resist breakdown by hydrogen and thereby decrease the propensity to form methane [6]. The solid-line curves in Figure 1 reflect the increased resistance to internal attack when molybdenum and chromium are present.

The presence of nonmetallic inclusions tends to increase the extent of blistering damage. If steel contains segregated impurities, stringer-type inclusions or laminations then severe blistering may in these areas from hydrogen or methane accumulation [7].

Alloys other than those shown in Figure 1 may also be suitable for resisting HTHA. These include modified carbon steels and low alloy steels to which carbide stabilizing elements (molybdenum, chromium, vanadium, titanium, or niobium) have been added such as some European alloys [8]. Austenitic stainless steels are resistant to decarburization, even at temperatures above 1000 °F (538 °C) [9].

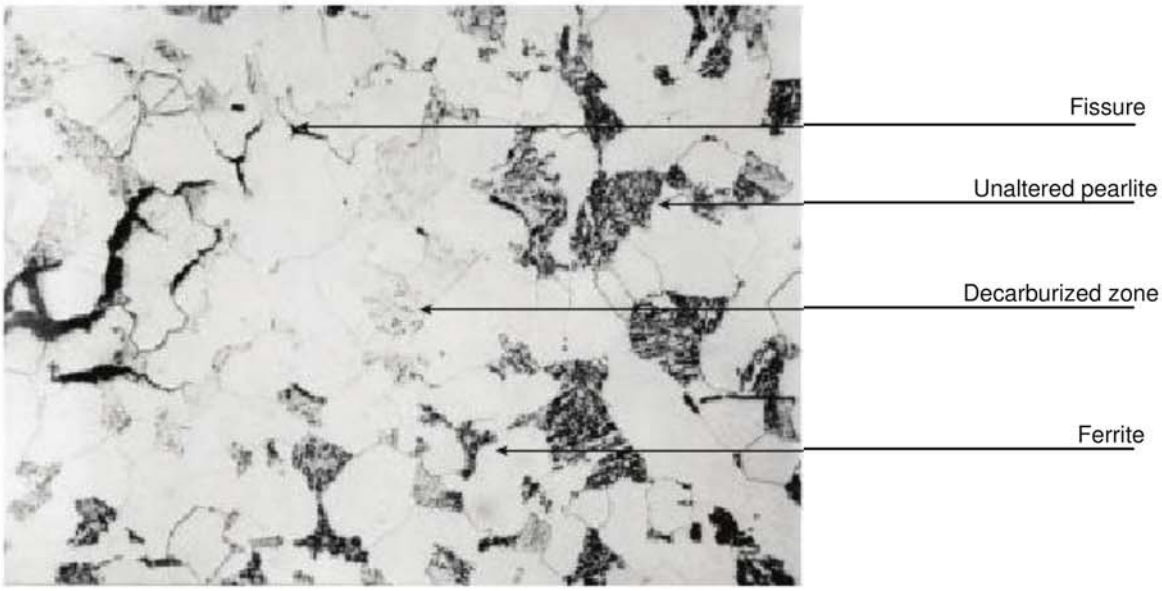

NOTE Service conditions were 65,000 hours in a catalytic reformer at a temperature of 790 °F (421 °C) and a hydrogen partial pressure of 425 psia (2.9 MPa). From Reference [11] in the Bibliography. Magnification: 520X; nital etched.

Figure 2—C-0.5Mo Steel (ASTM A204 Grade A) Showing Internal Decarburization and Fissuring in High Temperature Hydrogen Service

5 Factors Influencing Internal Decarburization, Fissuring, and Cracking Caused by HTHA

5.1 Incubation Time

Internal HTHA begins once the service conditions (high pressure and high temperature hydrogen) are such that the hydrogen diffused into the steel begins to react with the carbon or carbides in the steel. In the initial stages of attack, there is a period of time where the damage is so microscopic that it cannot be detected by current nondestructive examination (NDE) and metallographic technology. Beyond this there is also a period when no noticeable change in mechanical properties is detectable by current testing methods. After this period of time has elapsed, material damage is evident with resultant decreases in strength, ductility, and toughness. This varies with the type of steel and severity of exposure; it may take only a few hours under extreme conditions and take progressively longer at lower temperatures and hydrogen partial pressures. With some steels under mild conditions, no damage can be detected even after many years of exposure. During this initial stage of attack, in some cases, laboratory examination (high magnification metallography, utilizing optical microscopy and scanning electron microscopy) of samples removed from the equipment have revealed the initial stages of attack with voids at grain boundaries.

The period of time until mechanical damage can be detected is commonly referred to as the “incubation time” in the petrochemical industry. The length of the incubation period is important because it determines the useful life of a steel at conditions under which internal HTHA occurs. Useful theoretical models of the HTHA mechanism and incubation period have been proposed [11] [12] [13] [39].

Internal HTHA can be viewed as occurring in four stages:

a) the incubation period during which the microscopic damage cannot be detected with advanced NDE techniques and the mechanical properties are not affected;

b) the stage where damage is detectable optically (<1000X), possibly detectable by advanced NDE techniques, and mechanical properties are partially deteriorated;

c) the stage of rapid mechanical property deterioration associated with rapid fissure growth; and

d) the final stage where carbon in solid solution is reduced to compromise material mechanical properties to a level where cracking can occur.

During the incubation period, methane pressure builds up in submicroscopic voids. These voids grow slowly due to both internal methane pressure and applied stress. When the voids reach a critical size and begin connecting to form fissures, the effects on mechanical properties become evident. The incubation period depends on many variables including the type of steel, degree of cold working, amount of impurity elements, applied stress, hydrogen pressure, and temperature.

Incubation curves for non-welded or welded with PWHT carbon steel are given in Figure 3. These can be used as a guide in determining approximate safe operating times when PWHT'd carbon steel equipment operates above its curve in Figure 1. Annex A includes similar curves that may be useful for some heats of C-0.5Mo steel, with the precaution that the resistance of C-0.5Mo steel to HTHA is particularly sensitive to heat treatment, chemical composition, and the heating/cooling history of the steel during forming [15] [16] [17] [18]. API Technical Report (TR) 941, *The Technical Basis Document for API RP 941*, provides additional guidance on safe operating times for steels above their respective curves in Figure 1.

The Figure 3 [14] and Annex A incubation curves, as well as the guidance in API TR 941, are commonly used to evaluate unintentional upsets and short-term intentional operating periods such as during start-up of a process unit and elevated temperatures at end of run. Recent experience with HTHA in liquid-filled hydrocarbon service showed that HTHA occurred much more rapidly than what these curves predict. Incubation curves should not be used for liquid-filled streams.

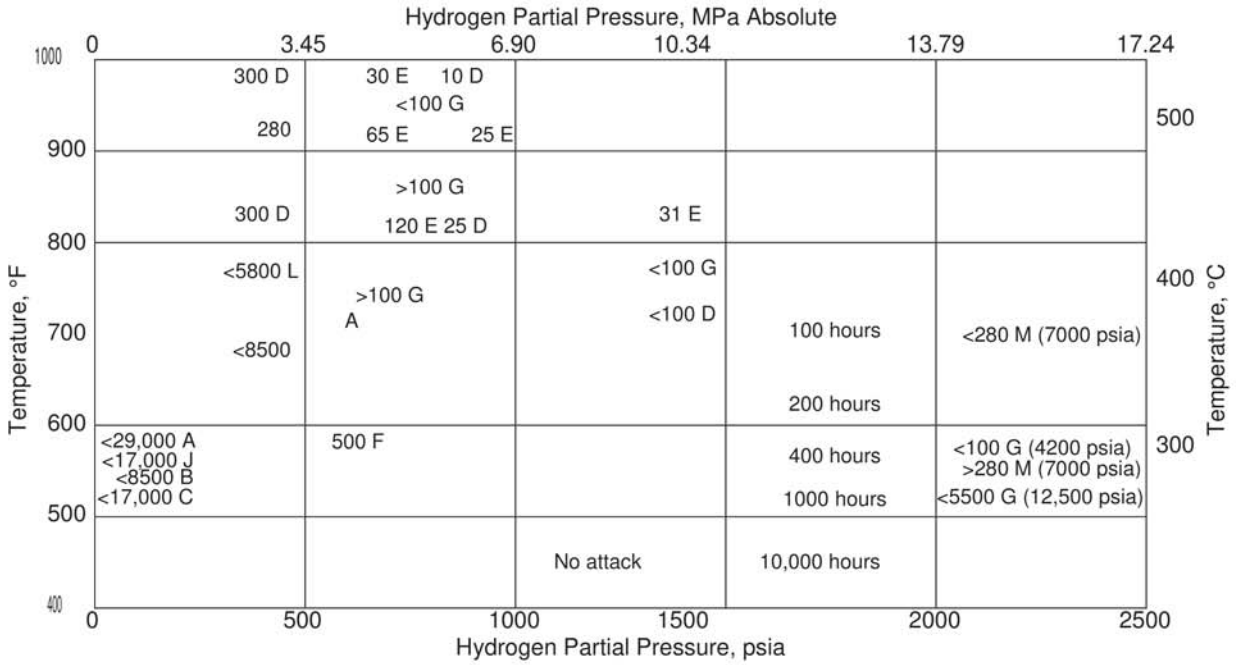

NOTE 1 the letter "I" is not used

NOTE 2 This figured first appeared as Figure 4 in the first edition (1970) of this publication.

NOTE 3 See Section 6.2 for references related to this figure.

Figure 3—Incubation Time for High Temperature Hydrogen Attack Damage of Carbon Steel (Non-welded or Welded with Postweld Heat Treatment) in High Temperature Hydrogen Service

5.2 Effect of Primary Stresses

Primary stresses are design stresses imposed by internal pressure, nozzle loadings, and the like. While it is known that very high stress levels can accelerate the rate of HTHA development (see, for example, Annex C), long-term operating experience dating from before 1969 has demonstrated that equipment designed within the allowable stresses of the relevant ASME Codes, which include ASME Section VIII Divisions 1 and 2 for pressure vessels and ASME B31.3 for piping, as well as equivalent foreign national codes, will perform satisfactorily when operated within the temperature and hydrogen partial pressure limits given in Figure 1 for the particular steel.

ASME Section VIII Division 2 has higher allowable design stresses than Division 1 and is typically used for high pressure, high temperature, thick-wall pressure vessels made of Cr-Mo steels. The Cr-Mo steels typically receive a normalized and tempered (N&T) or quenched and tempered (Q&T) heat treatment to provide improved fracture toughness, as well as slightly higher strength, as compared to carbon steel. Cr-Mo steel vessels designed to the higher allowable stress levels of Division 2 have a long, successful history of resistance to HTHA, as long as stresses are within the ASME Code allowable limits (or similar allowable limits in equivalent non-ASME Codes) and when operated within the temperature and hydrogen partial pressure limits given in Figure 1. This is evidenced by the lack of internal decarburization and fissuring data points for the steels in Figure 1.

While unusually high localized stresses have, in rare cases, caused HTHA in 2.25Cr-1Mo steel under temperature and hydrogen partial pressure conditions not expected to cause damage according to Figure 1 [23], there is no report of HTHA below the Figure 1 limits when stresses are within the design limits of the ASME Code.

Research studies [19] [20] [21] [22] have shown that creep strength and ductility of 2.25Cr-1Mo steel are diminished in very high pressure H_2 as compared to air. However, as long as operating temperatures are kept below the 850 °F (454 °C) limit given in Figure 1, creep of 2.25Cr should not be an issue.

5.3 Effect of Secondary Stresses

HTHA can be accelerated by secondary stresses such as thermal stresses or those induced by cold work. High thermal stresses were considered to play a significant role in the HTHA of some 2.25Cr-1Mo steel piping [24]. Other 2.25Cr-1Mo steel piping in the same system, subjected to more severe hydrogen partial pressures and temperatures, was not attacked.

The effect of cold work was demonstrated by Vitovec in research sponsored by API and summarized in API 940 [6]. Vitovec compared specific gravities of SAE 1020 steel with varying degrees of cold work tested in 900 psi (6.2 MPa) hydrogen at 700 °F (371 °C), 800 °F (427 °C), and 1000 °F (538 °C). The decrease in specific gravity over time indicates the rate at which internal fissures are produced by HTHA. Annealed samples (0 % strain) had an incubation period followed by a decrease in specific gravity. Steels with 5 % strain had shorter incubation periods and specific gravity decreased at a more rapid rate. Steels with 39 % strain showed no incubation period at any test temperature, indicating that fissuring and cracking started immediately upon exposure to hydrogen.

These tests are considered significant in explaining the cracks sometimes found in highly stressed areas of an otherwise apparently resistant material. In addition, Cherrington and Ciuffreda [25] have emphasized the need for removing notches (stress concentrators) in hydrogen service equipment.

5.4 Effect of Heat Treatment

Both industry experience and research indicate that PWHT of steels (carbon steels, C-0.5Mo steels and chromium-molybdenum steels) in hydrogen service improves resistance to HTHA. The PWHT stabilizes alloy carbides. This reduces the amount of carbon available to combine with hydrogen, thus improving HTHA resistance. Also, PWHT reduces residual stresses and is, therefore, beneficial for all steels.

Research [4] [13] [17] [18] [26] has shown that certain metal carbides may be more resistant to decomposition in high temperature hydrogen environments. Creep tests in hydrogen demonstrated the beneficial effect of increased PWHT on the HTHA resistance of 2.25Cr-1Mo steel [19]. In these tests, 2.25Cr-1Mo steels PWHT'd for 16 hours at 1275 °F

(691 °C) showed more resistance to HTHA than the same steels PWHT'd for 24 hours at 1165 °F (630 °C). While PWHT for longer duration showed some beneficial effect, high PWHT temperatures have a more beneficial effect on HTHA resistance. Similarly, HTHA resistance of 1Cr-0.5Mo and 1.25Cr-0.5Mo steels is improved by raising the minimum PWHT temperature to 1250 °F (677 °C) from the 1100 °F (593 °C) minimum required by past additions of Section VIII of the ASME Code.

The user must balance the advantages of high PWHT temperatures with other factors such as the effect upon strength and notch toughness.

NOTE Note higher PWHT temperatures can affect the ability to meet ASME Code Class 2 strength requirements, and the strength requirements of enhanced grades of low alloy steels.

Local PWHT bands often do not effectively reach desired temperatures throughout the weldment. In order to improve the effectiveness of PWHT, the band widths shall be increased as recommended by American Welding Society (AWS) D10.10 for piping and Welding Research Council (WRC) 452 for vessels. For each PWHT, three different band widths are specified in these standards, namely soak band, heating band, and gradient control band. The recommended thermocouple placements in these standards shall also be followed.

5.5 Effect of Stainless Steel Cladding or Weld Overlay

The solubility of hydrogen in austenitic stainless steel is about an order of magnitude greater than for ferritic steels [27]. The diffusion coefficient of hydrogen through austenitic stainless steel is roughly two orders of magnitude lower than for ferritic steels [28] [29] [39]. This can result in a significant reduction in the effective hydrogen partial pressure experienced by the underlying steel below the cladding.

Ferritic or martensitic stainless steel (400 Series) claddings or weld overlays have similar solubilities and diffusivities than the underlying ferritic steel [39] [41]. As a result, the only reduction in hydrogen partial pressure realized for ferritic or martensitic cladding is roughly equal to the ratio of the cladding to the base metal as follows:

$$P_{eff} = P_{H2}\left(\frac{t_{base\ metal}}{t_{base\ metal} + t_{cladding}}\right)$$

where

P_{H2} is the hydrogen partial pressure,

P_{eff} is the effective hydrogen partial pressure,

$t_{base\ metal}$ is the thickness of base metal,

$t_{cladding}$ is the thickness of clad/overlay.

A sound metallurgically bonded austenitic stainless steel cladding or weld overlay can significantly reduce the effective hydrogen partial pressure acting on the base metal. The amount of hydrogen partial pressure reduction depends upon the materials and the relative thickness of the cladding/weld overlay and the base metal. The thicker the stainless steel barrier is relative to the base metal, the lower the hydrogen concentration [30] [39]. Archakov and Grebeshkova [31] mathematically considered how stainless steel corrosion barrier layers increase resistance of carbon and low alloy steels to HTHA. The calculation for determining the effective hydrogen pressure at the clad/weld overlay-to-base metal interface is presented in Annex D.

There have been a few instances of HTHA of base metal that was clad or overlayed with austenitic stainless steel. All of the reported instances involved C-0.5Mo steel base metal. In one case [32], HTHA occurred in a reactor vessel at a nozzle location where the C-0.5Mo base metal was very thick, relative to the cladding/overlay. Another incident of HTHA of C-0.5Mo steel occurred under intergranularly cracked Type 304 austenitic stainless steel cladding (see data point 51U in Annex A). The other cases involved ferritic or martensitic stainless steel cladding.

It is not advisable to take a credit for the presence of a stainless steel cladding/weld overlay when selecting the base metal for a new vessel. Some operators have successfully taken credit for the presence of an austenitic stainless steel cladding/weld overlay for operation when conditions exceeded the Figure 1 curve for the base metal. Satisfactory performance in such cases requires assurance that the effective hydrogen partial pressure acting on the base metal be accurately determined and that the integrity of the cladding/weld overlay be maintained. Such assurance may be difficult to achieve, especially where complex geometries are involved. Many operators take the presence of an austenitic stainless steel cladding/weld overlay into account when establishing inspection priorities for HTHA, especially for C-0.5Mo steel equipment.

More background information and details about many of these factors can be found in API TR 941 [39].

6 Inspection for HTHA

6.1 The selection of optimum inspection methods and intervals for HTHA in specific equipment or applications is the responsibility of the owner/user. The information below and Tables E.1a–E.2 are intended to assist the owner/user in making such decisions. Estimating the damage rate and assessing fitness-for-service based on inspection results requires an advanced level of analysis. Specialized expertise required to correlate NDE data with HTHA damage state is necessary, and an update to API 579-1 is being developed to provide guidance for estimating damage rates and life assessment.

6.2 Most owner/users do not inspect equipment for HTHA damage unless it has been operated near or above the associated material in Figure 1. An HTHA inspection program should also consider equipment that operates infrequently above its curve (e.g. operations such as “hot hydrogen stripping” in hydroprocessing reactors and associated piping and equipment).

6.3 Only a small number of documented instances of HTHA occurring at conditions below the Figure 1 operating limit curves have been reported to API (see Annex A, Annex B, Annex C and Annex F). Most of these have involved C-0.5Mo steel [33] or non-PWHT’d carbon steel [40]. Periodic inspection of C-0.5Mo steel equipment and piping should be considered if operated above the carbon steel curve, based on factors such as relative position of the operating parameters versus the carbon steel curve, consequence of failure, presence of cladding (and the type and condition of that cladding), prior heat treatment, etc. Because it is time dependent, existing C-0.5Mo steel equipment and piping may continue to deteriorate with time, if susceptible.

6.4 As this equipment and piping age, the probability of HTHA damage increases, and the owner should consider increasing the inspection frequency (also see Annex A).

6.5 HTHA damage may occur in welds, weld HAZs, or in the base metal. Even within these specific areas, the degree of damage may vary widely. Consequently, if damage is suspected, then a thorough inspection of representative samples of these areas should be conducted. The inspection scope should be determined by owner’s subject matter experts (SMEs).

6.6 Tables E.1a-E.2 provide a summary of available methods of inspection for HTHA damage and include a discussion of the advantages and limitations of each. Encoded ultrasonic testing (UT) techniques as described in Table E.1a are effective for detecting HTHA damage, and two or more recommended UT techniques are often used in combination to overcome the limitations of any single technique. High sensitivity (HS) wet fluorescent magnetic testing (WFMT) can detect early stages of HTHA damage. See E.3.4 for further description of HSWFMT. HTHA damage detection using HSWFMT is limited to the depth of removed material and highly dependent surface preparation. Metal sample removal and metallurgical analysis is the most effective method for characterization and improving NDE interpretation.

6.7 HTHA inspections can be challenging. The early stages of attack with fissures, or even small cracks, can be difficult to differentiate from metallurgical imperfections, creep, or other cracking mechanisms. The advanced stage of attack, with significant cracking, is much easier to detect, but at that point there is already a higher likelihood of equipment failure. In addition to attack of the base metal, HTHA has been known to occur as a very narrow band of

concentrated damage and cracking, transverse and/or parallel to welds (see Figure E.3). It should be noted that large cracks can be masked by the presence of microdamage, and this can result in nondetection by both reflective and diffraction-based ultrasonic techniques. The long-term operation of equipment with known HTHA damage that is ongoing and progressing is not advisable when managed only by periodic NDE.

6.8 Of all the inspection methods for base metal examination, UT techniques and HSWFMT are the most sensitive techniques and have the best chance of detecting HTHA damage while still in the fissuring stage, prior to the onset of significant cracking. The most recent approach is a combination of time of flight diffraction (TOFD), phased array UT (PAUT), and/or full matrix capture/total focusing method (FMC/TFM). The new combined approach is considered to be more effective than the previous approach (i.e. advanced ultrasonic backscatter technique [AUBT] contained in the prior edition of API RP 941). AUBT has limited data recording capability and is highly dependent upon technician training and usage of the proper procedure. Manual scanning techniques (without data recording) should only be considered as a supplement for HTHA detection when encoded data recording is not possible.

6.9 When the internal surface is accessible, HSWFMT can be used to detect surface-breaking fissures while WFMT is limited to the detection of surface-breaking cracks. HSWFMT has significant surface preparation requirements that are reviewed in the “new approaches” section of Annex E. Close visual inspection can detect small, coin-sized surface blisters, which can be an indication of the presence of internal HTHA. Visual inspection for HTHA damage requires a very close examination using light sources capable of being directed at oblique angles on to the surface being examined, permitting observation of shadows created by blistering. The absence of surface blisters does not provide assurance that internal HTHA is not occurring, since HTHA frequently occurs without the formation of surface blisters.

6.10 Field metallography and replication (FMR), also called in-situ metallography, can be effective in detecting the early stages of HTHA (decarburization and fissuring) at the surface of the steel as well as differentiating between HTHA and other forms of cracking and naturally occurring inclusions in the steel. Skill and experience are required for the surface polishing, etching, replication, and microstructural interpretation. A triple etch/polish procedure is recommended (similar to creep evaluations) to reveal the fine details of HTHA damage so that accurate identification of HTHA can be made. After the final polish step, the surface should be lightly etched so that individual fissures and voids are not obscured by the grain boundaries. Because in situ metallography only examines one surface at a time, in order to evaluate a cross section of damage, either multiple replicas need to be taken at different depths of grinding or the depth can be varied by tapering the grinding so that the replica can extend from shallow to deeper locations of the prepared location. Metallurgical sampling (e.g. “scoop” or “boat” sampling) has the advantage of capturing a cross section and some length of material that can be examined in a metallurgical lab. Metallographic examination should be used to better interpret NDE results and damage classification. One note of caution is that HTHA may be subsurface, so using a surface inspection technique, such as replication or WFMT, may not detect damage. Since HTHA fissuring begins subsurface, it is recommended to remove 0.020 in. to 0.120 in. (0.5 mm to 3 mm) of material during the preparation for FMR examination. If desired, more material can be removed to reveal damage further subsurface or to confirm the depth of damage that was indicated by NDE techniques.

Annex A
(informative)

HTHA of 0.5Mo Steels

A.1 General

The purpose of this annex is to provide a brief summary of the information and experience regarding the use of 0.5Mo (C-0.5Mo and Mn-0.5Mo) steels in elevated temperature and pressure hydrogen service.

Most companies no longer specify C-0.5Mo steel for new or replacement equipment used for operation above the PWHT'd carbon steel curve in Figure 1 because of the uncertainties regarding its performance after prolonged use. Since 1970, a series of unfavorable service experiences with C-0.5Mo steels has reduced confidence in the position of the 0.5Mo curve [40] [41]. In the Second Edition (1977) of this publication, the 0.5Mo curve was lowered approximately 60 °F (33 °C) to reflect a number of plant experiences that involved HTHA of C-0.5Mo equipment. In the Fourth Edition (1990) of this publication, the 0.5Mo curve was removed from Figure 1 due to additional cases of HTHA of C-0.5Mo steel equipment occurring by as much as 200 °F (111 °C) below the curve. At that time, experience had identified 27 instances of HTHA below the 1977 curve. The operating conditions for these instances are given in Table A.1 and are plotted on Figure A.1.

No instances of HTHA have been reported using Mn-0.5Mo steel operating below the Figure A.1 0.5Mo curve. The information and use of this material at elevated temperatures and hydrogen partial pressures are limited.

C-0.5Mo steels vary in their resistance to HTHA. Many heats seem to have resistance at conditions indicated by the 0.5Mo curve in Figure A.1. However, some heats seem to have HTHA resistance only marginally better than carbon steel. Published works [41] [42] [43] [44] suggest a correlation between thermal history of the steel and its resistance to HTHA. Slow-cooled, annealed C-0.5Mo steels have less resistance to HTHA than normalized steels. The studies have shown that PWHT improves the HTHA resistance of weldments and HAZs for both annealed and normalized C-0.5Mo steels. However, the base metals of slow-cooled, annealed C-0.5Mo steels show a decrease in HTHA resistance after PWHT. The initial studies suggest that this is due to free carbon being present in the ferrite matrix after PWHT. Normalized C-0.5Mo steel base metals, on the other hand, show improvement in HTHA resistance following tempering or PWHT. Such normalized and PWHT'd C-0.5Mo steel appears to have hydrogen attack resistance about as indicated by the 0.5Mo curve in the Second Edition (1977) of this publication. Until the factors controlling the HTHA resistance of C-0.5Mo are better understood, each user should carefully assess the use of C-0.5Mo steel in services above the PWHT'd carbon steel curve in Figure 1.

Existing C-0.5Mo steel equipment that is operated above the PWHT'd carbon steel curve in Figure 1 should be inspected to detect HTHA. Owners/operators should evaluate and prioritize for inspection C-0.5Mo equipment operating above the carbon steel limit—Hattori and Aikawa [45] addressed this issue. The work cited above and plant experience suggest that important variables to consider in prioritizing equipment for inspection include severity of operating condition (hydrogen partial pressure and temperature), thermal history of the steel during fabrication, stress, cold work, and cladding composition and thickness, when present.

To provide a historical summary of the data regarding the use of C-0.5Mo steels, two additional figures are included here:

a) Figure A.2, which shows the effect of trace alloying elements and molybdenum on PWHT'd carbon steel operating limits; and

b) Figure A.3, which shows HTHA incubation times for C-0.5Mo steels.

Figure A.2 is from the second edition of this publication (1977) and is a revision of a similar figure from the original edition (1970). Figure A.2 shows that molybdenum has long been considered to be beneficial to the HTHA resistance

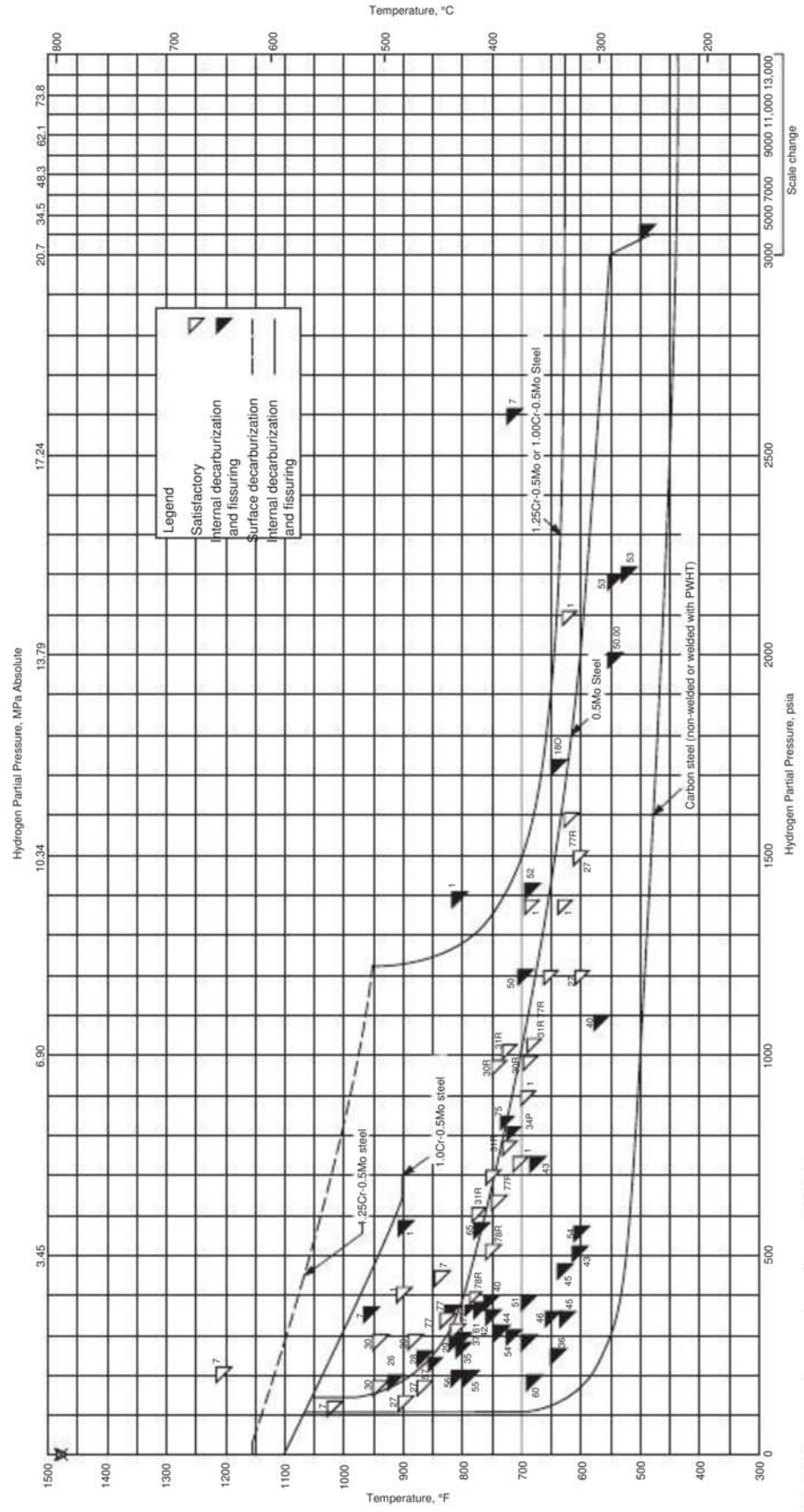

NOTE 1 References and comments are shown on Table A.1.

NOTE 2 Curves for carbon steel, 1.0Cr-0.5Mo steel, and 1.25 Cr-0.5Mo steel are included for reference.

NOTE 3 The symbol is retained as a reference against previous editions of this publication.

NOTE 4 Reference numbers are the same as in previous editions of this publication.

NOTE 5 The 0.5Mo steel curve is the same as the one shown in the Seventh Edition of this publication (2008).

Figure A.1—Experience with C-0.5Mo and Mn-0.5Mo Steel in High Temperature Hydrogen Service

of steels. The data in Figure A.3 should be used with caution, since some heats of C-0.5Mo steels have suffered HTHA during exposure to conditions under the lower solid curve (equivalent to the C-0.5Mo curve of Figure A.1). The data for the instances of HTHA listed in Table A.1 and plotted on Figure A.1 are also shown for reference in Figure A.3. In these cases, the service life at the time the attack was detected was less than the incubation time indicated by the curves, which, of course, is not possible.

A.2 Section A.1 References

40) R.D. Merrick and A.R. Ciuffreda, “Hydrogen Attack of Carbon-0.5-Molybdenum Steels,” *1982 Proceedings*, *Refining Department*, Vol. 61, API, Washington, DC, pp. 101–114.

41) M.C. Maggard, “Detecting Internal Hydrogen Attack,” *Oil & Gas Journal*, pp. 90–94, Mar. 10, 1980.

42) K. Ishii, K. Maeda, R. Chiba, and K. Ohnishi, “Intergranular Cracking of C-0.5Mo Steel in a Hydrogen Environment at Elevated Temperatures and Pressures,” *1984 Proceedings*, *Refining Department*, Vol. 63, API, Washington, DC, pp. 55–64.

43) R. Chiba, K. Ohnishi, K. Ishii, and K. Maeda, “Effect of Heat Treatment on the Resistance of C-0.5Mo Steel Base Metal and Its Welds to Hydrogen Attack,” *1985 Proceedings, Refining Department*, Vol. 64, API, Washington, DC, pp. 57–74.

44) T. Ishiguro, K. Kimura, T. Hatakeyama, T. Tahara, and K. Kawano, “Effect of Metallurgical Factors on Hydrogen Attack Resistance in C-0.5Mo,” presented at the Second International Conference on Interaction with Hydrogen in Petroleum Industry Pressure Vessel and Pipeline Service, Materials Properties Council, Vienna, Austria, Oct. 19–21, 1994.

45) K. Hattori and S. Aikawa, “Scheduling and Planning Inspection of C-0.5Mo Equipment Using the New Hydrogen Attack Tendency Chart,” PVP-Vol. 239/MPC-Vol. 33, *Serviceability of Petroleum Process and Power Equipment*, ASME, 1992.

A.3 References and Comments for Figure A.1

NOTE The data in Figure A.1 are labeled with the reference numbers corresponding to the sources listed below. The letters in the figure correspond to the comments listed on this page.

A.3.1 Figure A.1 References

1) Shell Oil Company, private communication to API Subcommittee on Corrosion.

7) Standard Oil Company of California, private communication to API Subcommittee on Corrosion.

18) Union Oil Company of California, private communication to API Subcommittee on Corrosion, 1980.

27) Union Oil Company of California, private communication to API Subcommittee on Corrosion, 1976.

28) Amoco Oil Company, private communication to API Subcommittee on Corrosion, 1976.

29) Standard Oil Company of California, private communication to API Subcommittee on Corrosion, 1976.

30) Exxon Corporation, private communication to API Subcommittee on Corrosion, 1976.

31) Shell Oil Company, private communication to API Subcommittee on Corrosion, 1976.

32) Cities Service Company, private communication to API Subcommittee on Corrosion, 1976.

34) Koch Refining Company, private communication to API Subcommittee on Corrosion, 1980.

36) [A]Texaco Incorporated, private communication to API Subcommittee on Corrosion, 1980.

37) [B]Exxon Corporation, private communication to API Subcommittee on Corrosion, 1979.

38) [C]Exxon Corporation.

39) [D]Exxon Corporation.

41) [F]Caltex Petroleum Corporation, private communication to API Subcommittee on Corrosion, 1980.

42) [G]Getty Oil Company.

43) [H]Getty Oil Company.

44) [I]Caltex Petroleum Corporation, private communication to API Subcommittee on Corrosion and Materials Engineering, 1984.

45) [J]JGC Corporation/Japan Steel Works, API Midyear Refining Meeting, 1984.

46) [K,E]JGC Corporation/Japan Steel Works, Exxon Corporation.

47) [L]JGC Corporation/Japan Steel Works, API Midyear Refining Meeting, 1985.

48) [M]Air Products & Chemicals, Inc., private communication to API Subcommittee on Corrosion and Materials Engineering, 1985.

49) [S]Texaco USA, API Fall Refining Meeting, 1985.

50) [T]Mobil R&D Corporation, private communication to API Subcommittee on Corrosion and Materials Engineering, 1986.

51) [U]Shell Oil Company, private communication to API Subcommittee on Materials Engineering and Inspection, 1987.

52) [V]Texaco, Inc., private communication to API Subcommittee on Corrosion, 1981.

53) Kemira, B. V., private communication to API Subcommittee on Materials Engineerings and Inspection, 1986.

54) [AA]Chevron Research and Technology Company, private communication to API Subcommittee on Corrosion and Materials, June 1992.

55) [BB]Chevron Research and Technology Company, private communication to API Subcommittee on Corrosion and Materials, June 1992.

56) [CC]Chevron Research and Technology Company, private communication to API Subcommittee on Corrosion and Materials, June 1992.

57) [DD]Chevron Research and Technology Company, private communication to API Subcommittee on Corrosion and Materials, June 1992.

58) [EE]Chevron Research and Technology Company, private communication to API Subcommittee on Corrosion and Materials, June 1992.

59) FFChevron Research and Technology Company, private communication to API Subcommittee on Corrosion and Materials, June 1992.

60) GGChevron Research and Technology Company, private communication to API Subcommittee on Corrosion and Materials, June 1992.

61) HHChevron Research and Technology Company, private communication to API Subcommittee on Corrosion and Materials, June 1992.

62) IIChevron Research and Technology Company, private communication to API Subcommittee on Corrosion and Materials, June 1992.

63) JJTosco, private communication to API Subcommittee on Corrosion and Materials, April 1993.

64) KKTosco, private communication to API Subcommittee on Corrosion and Materials, April 1993.

65) LLExxon report: “Hydrogen Attack of Gofiner Reactor Inlet Nozzle,” 1988.

A.3.2 Figure A.1 Comments

A) Feed line pipe leaked; isolated areas damaged. Blistered, decarburized, fissured; PWHT’d at 1100 °F to 1350 °F.

B) Effluent line, pipe and HAZ, isolated areas damaged; no PWHT.

C) Weld and pipe, isolated areas damaged; no PWHT.

D) Effluent line; weld, isolated areas damaged; PWHT.

E) Feed line; weld and HAZ, isolated areas damaged; PWHT.

F) Feed/effluent exchanger nozzle-to-shell weld, cracks in welds and in exchanger tubes.

G) Effluent exchanger channel; welds, plate, and HAZ, isolated areas damaged; PWHT.

H) Effluent exchanger channel; welds, plate, and HAZ, isolated areas damaged; PWHT’d at 1100 °F.

I) Catalytic reformer, combined feed/effluent exchanger shell; plate; PWHT’d at 1250 °F.

J) Hydrodesulfurization unit effluent exchanger channel head and shell plate. (Hydrocarbon feed to unit and makeup hydrogen from ethylene unit.)

K) Catalytic reformer combined feed piping; welds and base metal; PWHT.

L) Gas-oil hydrodesulfurization unit. Elbow cracked intergranularly and decarburized at fusion line between weld metal and HAZ; no PWHT.

M) Ammonia plant converter; exit piping; intergranular cracking and internal decarburization of pipe.

P) Hydrodesulfurization unit hydrogen preheat exchanger shell; blisters, intergranular fissuring, and decarburization in weld metal; PWHT’d at 1150 °F.

Q) Attack of heat exchanger tubing in tubesheet.

R) Stainless steel cladding on 0.5Mo steel; no known HTHA.

S) Decarburization and fissuring of weld metal; PWHT'd at 1150 °F.

T) Forged tubesheet cracked with surface decarburization; tubes blistered.

U) Hydrodesulfurization unit, C-0.5Mo steel exchanger tubesheet; decarburized, fissured, and cracked under intergranularly cracked ASTM Type 304 cladding.

V) Hydrocracker charge exchanger liquid with a small amount of hydrogen; C-0.5Mo with Type 410S rolled bond clad. Extensive blistering and fissuring under clad.

W) C-0.5Mo steel piping in ammonia plant syngas loop; decarburized and fissured.

AA) Blistering and fissuring of a flange.

BB) HAZ and base metal fissuring of pipe.

CC) Base metal fissuring and surface blistering in heat exchanger shell.

DD) Attack at weld, HAZ and base material in piping.

EE) Localized attack in weld, HAZ in piping.

FF) Base metal attack in piping.

GG) Base metal attack in a heat exchanger channel.

HH) Base metal attack in piping.

II) Blistering and base metal attack in a heat exchanger shell.

JJ) Base metal attack in a TP405 roll bond clad vessel.

KK) Base metal attack in a TP405 roll bond clad vessel.

LL) Attack in nozzle attachment area of a vessel weld overlaid with Type 309Nb.

MM) Internal decarburization/fissuring of piping in a hydrocracker unit after 235,000 hours of service.

Table A.1—Operating Conditions for C-0.5Mo Steels That Experienced High Temperature Hydrogen Attack Below the 0.5Mo Steel Curve in Figure A.1

Point	Temperature		Hydrogen Partial Pressure (Absolute)		Service Hours (Approximate)	Degrees Below 0.5Mo Curve (Approximate)	
	°F	°C	psi	MPa		°F	°C
36A [a]	790	421	350	2.41	80,000	20	11
37B [a]	800	427	285	1.97	57,000	30	17
38C [a]	640	338	270	1.86	83,000	180	100
39D [a]	700	371	300	2.07	96,000	125	69
41F [a]	760	404	375	2.59	85,000	40	22
42G [a]	750	399	350	2.41	150,000	60	33
43H [a]	625	329	350	2.41	150,000	185	103
44I [a]	730 [b]	388 [b]	313	2.16	116,000	90	50
45J [c]	620/640	327/338	457	3.15	70,000	167/147	93/82
46K [a]	626/680	330/360	350	2.41	131,000	184/130	102/72
47L [c]	684 [b]	362	738	5.09	61,000	54	30
48M [e]	550/570	288/299	1060/1100	7.31/7.59	79,000	125/105	69/58
[f]	655/670	346/354	—	—	17,500	20/5	11/3
49S [c]	750/770	399/410	390	2.69	67,000	50/30	28/17
[f]	650	343	—	—	163,000	150	83
51U [c]	690	366	397	2.74	—	100	56
53W [e]	545	285	2190	15.1	140,000	45	25
54AA [a]	725/760	385/404	300/380	2.07/2.62	105,000	40/100	22/56
55BB [a]	800/850	427/454	175/190	1.21/1.31	124,000	80/30	44/17
56CC [a]	810/825	432/441	275/300	1.90/2.07	223,000	15/0	8/0
57DD [a]	850 [d]	454 [d]	225 [d]	1.55 [d]	158,000	10	6
58EE [a]	810/855	432/457	170	1.17	138,000	70/25	39/14
59FF [c]	550/600	288/316	2000	13.79	210,000	50/0	28/0
60GG [c]	550/600	288/316	2000	13.79	210,000	50/0	28/0
61HH [c]	530/600	277/316	2200	15.17	210,000	60/0	33/0
62II [c]	670/700	354/371	190	1.31	192,000	180/150	100/83
63JJ [c]	600/750	316/399	500	3.45	235,000	180/30	100/17
64KK [c]	600/770	316/410	525	3.62	283,000	170/0	94/0
65LL [c]	775	413	550	3.79	—	0	0

NOTE Numbers and letters in the first column (labeled “Point”) refer to references and comments for Figure A.1.

Where two numbers are given, the first number represents average operating conditions while the second number represents maximum operating conditions.

[a] Catalytic reformer service.

[b] Average.

[c] Hydrodesulfurizer service.

[d] Maximum.

[e] Ammonia plant.

[f] API task group currently resolving these points.

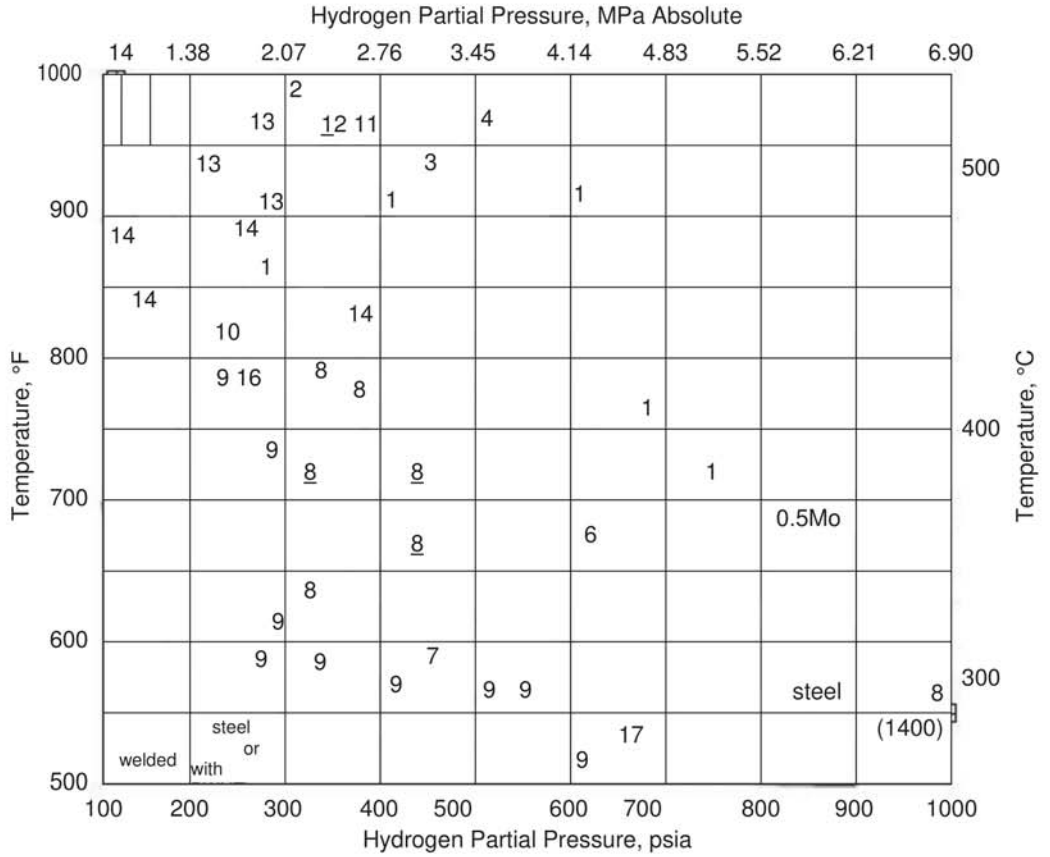

NOTE 1 Mo has four times the resistance of Cr to HTHA.

NOTE 2 Mo is equivalent to V, Ti, or Nb up to 0.1 %.

NOTE 3 Si, Ni, and Cu do not increase resistence.

NOTE 4 P and S decrease resistance.

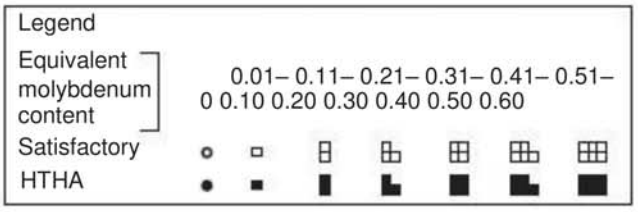

Figure A.2—Steels in High Temperature Hydrogen Service Showing Effect of Molybdenum and Trace Alloying Elements

A.4 References for Figure A.2

The data in Figure A.2 are labeled with the reference numbers corresponding to the sources listed in Table A.2.

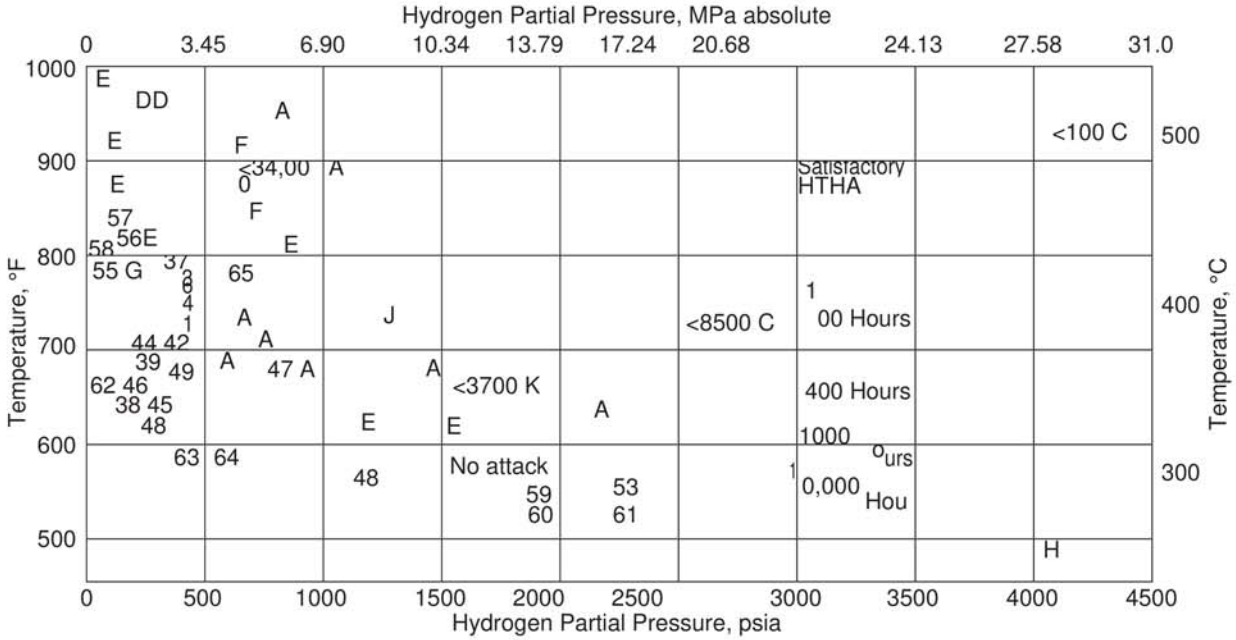

Figure A.3—Incubation Time for High Temperature Hydrogen Attack Damage of 0.5Mo Steels in High Temperature Hydrogen Service

Table A.2—References Along with Chromium, Molybdenum, Vanadium and Molybdenum Equivalent Values for Figure A.2

No.	Reference	Analysis			Mo Equiv.
		Cr	Mo	V	
1	Shell Oil Company[a]		0.50		0.50
2	Weld Deposits, D.J. Bergman[a]	0.79	0.39		0.59
3	Weld Deposits, D.J. Bergman[a]	0.80	0.15		0.35
4	Weld Deposits, D.J. Bergman[a]	0.50	0.25		0.37
5	Continental Oil Company[a]		0.25		0.25
6	Standard Oil Co. of California[a]		0.27		0.27
7	Standard Oil Co. of California[a]	0.05	0.06	0.08	
8	A.O. Smith Corp.[a]			0.13 to 0.18	0.11
9	Shell Development Co., Drawing No. VT 659-2				
10	Amoco Oil Company[a]	0.04			0.01
11	R.W. Manuel, Corrosion, *17*(9), pp. 103–104, Sept. 1961	0.27	0.15		0.22
12	The Standard Oil Co. of Ohio[a]	0.11	0.43		0.50
13	Exxon Corporation[a]				
14	Union Oil of California[a]				
15	Amoco Oil Company[a]				
16	Standard Oil Co. of California[a]				
17	Gulf Oil Corporation[a]				

[a] Private communication to Subcommittee on Corrosion (now Subcommittee on Corrosion and Materials).

Case	Temperature		Hydrogen Partial Pressure (Absolute)		Service Years	Description
	°F	°C	psi	MPa		
A	960	516	331	2.28	26	1.5 NPS Schedule 80 nozzle was broken off a catalytic reformer outlet line during a shutdown. Metallography indicated surface decarburization and intergranular cracking with bubbles. Cr content was 1.09 %.
B	977	525	354	2.44	14	Blistering was detected with ultrasonic examination in catalytic reformer piping. Metallography indicated surface decarburization and blistering at nonmetallic inclusions, with intergranular cracks growing from the blisters. Cr content was 1.10 %.
C	957/982	514/528	294/408	2.03/2.81	16	Blistering near pipe inner surface. Examination showed decarburization between the inner surface and the blister. Gas analysis indicated methane in the blister. Cr content was 1.12 %.
	See Note	See Note	See Note	See Note		

NOTE Average conditions are reported as the left number. Maximum condition reported as the right number.

Annex B
(informative)

HTHA of 1.25 Cr-0.5Mo Steel

The purpose of this annex is to provide a brief summary of the information and experience regarding three case histories with HTHA of 1.25Cr-0.5Mo steel.

Experiences with HTHA are listed in Table B.1 and the operating conditions are plotted in Figure B.1.

Table B.1—Experience with HTHA of 1.25Cr-0.5Mo Steel at Operating Conditions Below the Figure 1 Curve

No.	Reference	Analysis			Mo Equiv.
		Cr	Mo	V	
1	Shell Oil Company[a]		0.50		0.50
2	Weld Deposits, D.J. Bergman[a]	0.79	0.39		0.59
3	Weld Deposits, D.J. Bergman[a]	0.80	0.15		0.35
4	Weld Deposits, D.J. Bergman[a]	0.50	0.25		0.37
5	Continental Oil Company[a]		0.25		0.25
6	Standard Oil Co. of California[a]		0.27		0.27
7	Standard Oil Co. of California[a]	0.05	0.06	0.08	
8	A.O. Smith Corp.[a]			0.13 to 0.18	0.11
9	Shell Development Co., Drawing No. VT 659-2				
10	Amoco Oil Company[a]	0.04			0.01
11	R.W. Manuel, Corrosion, *17*(9), pp. 103–104, Sept. 1961	0.27	0.15		0.22
12	The Standard Oil Co. of Ohio[a]	0.11	0.43		0.50
13	Exxon Corporation[a]				
14	Union Oil of California[a]				
15	Amoco Oil Company[a]				
16	Standard Oil Co. of California[a]				
17	Gulf Oil Corporation[a]				

[a] Private communication to Subcommittee on Corrosion (now Subcommittee on Corrosion and Materials).

Cases A and B were reported by Chiyoda Corporation in Japan. Case C was originally reported by Merrick and Maguire of Exxon [7]. The mechanisms of attack were similar in Cases B and C. That is, damage was in the form of internal blistering with decarburization and intergranular cracking from the edges of the blisters. In Case A, however, attack resulted in intergranular separation. All three steels had chromium contents near 1.1 %, near the 1.0 % lower limit for 1.25Cr-0.5Mo steels. Additionally, the Case A steel had a relatively high impurity content with an X-bar equal to 31.5, as defined by Bruscato [38].

Case	Temperature		Hydrogen Partial Pressure (Absolute)		Service Years	Description
	°F	°C	psi	MPa		
A	960	516	331	2.28	26	1.5 NPS Schedule 80 nozzle was broken off a catalytic reformer outlet line during a shutdown. Metallography indicated surface decarburization and intergranular cracking with bubbles. Cr content was 1.09 %.
B	977	525	354	2.44	14	Blistering was detected with ultrasonic examination in catalytic reformer piping. Metallography indicated surface decarburization and blistering at nonmetallic inclusions, with intergranular cracks growing from the blisters. Cr content was 1.10 %.
C	957/982	514/528	294/408	2.03/2.81	16	Blistering near pipe inner surface. Examination showed decarburization between the inner surface and the blister. Gas analysis indicated methane in the blister. Cr content was 1.12 %.
	See Note	See Note	See Note	See Note		

NOTE Average conditions are reported as the left number. Maximum condition reported as the right number.

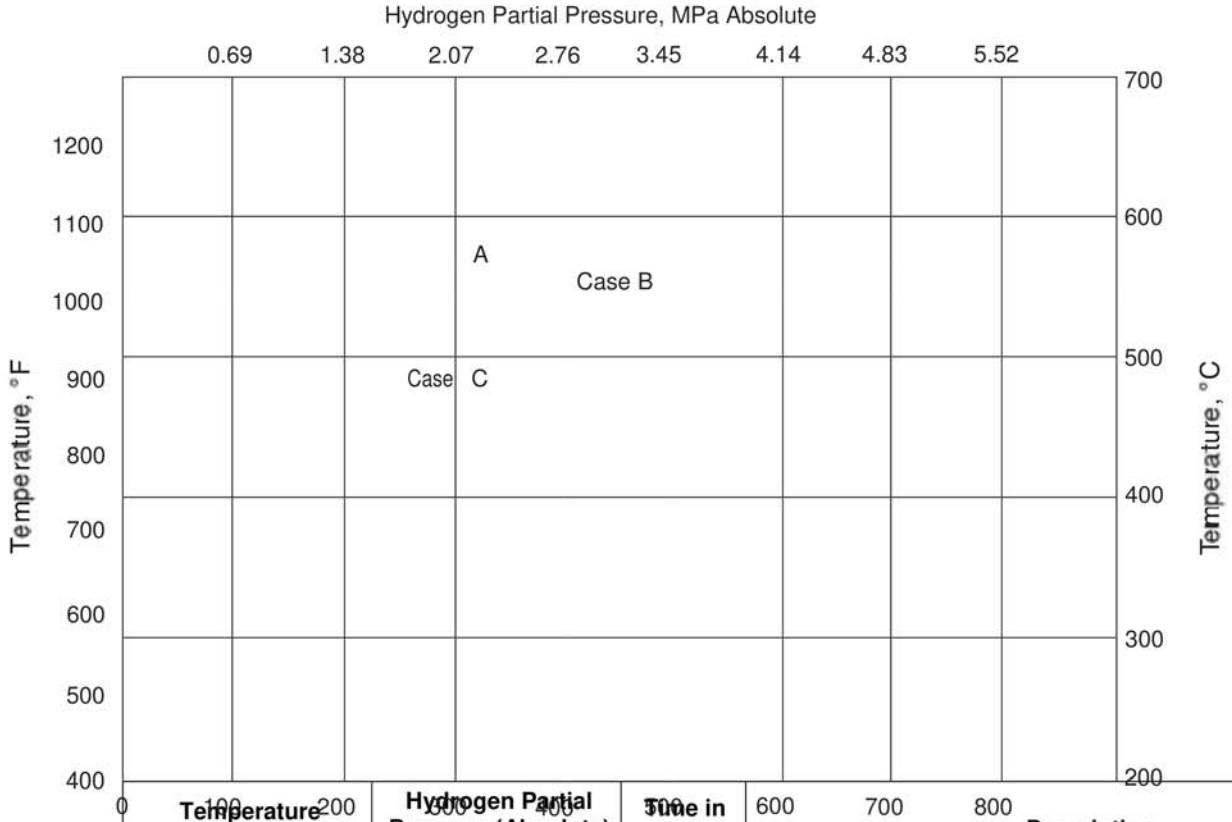

Figure B.1—Operating Conditions for 1.25Cr-0.5Mo Steels That Experienced High Temperature Hydrogen Attack Below the Figure 1 Curve

Temperature		Hydrogen Partial Pressure (Absolute)		Time in Service Years	Description
°F	°C	psi	MPa		
675/820	357/438	1385/1570	9.54/10.82	~20	A mixing tee for the hot and cold makeup hydrogen to a hydroprocessing unit leaked near the weld to the downstream piping. SEM examination indicated decarburization and fissuring along the internal surface of the tee.
See Note	See Note	See Note	See Note		Although the leak path was not positively identified, it was concluded to be most likely due to fine, interconnected fissures. Some thermal fatigue cracking was also identified in the tee. Piping downstream of the tee was also found to have fissuring and internal decarburization to a depth of about 3.90 mils (0.1 mm) along the inside surface. The hot, upstream piping was not found to be attacked.

NOTE Average conditions are reported as first number. Maximum condition reported as second number.

Annex C
(informative)

HTHA of 2.25Cr-1Mo Steel

The purpose of this annex is to provide a brief summary of experience regarding a case history [5] with HTHA of 2.25Cr-1Mo steel.

A recent experience with HTHA is described in Table C.1. This case history may indicate that highly stressed components can suffer HTHA at conditions below the curve in Figure 1. In this case history, a mixing tee was believed to be highly stressed by thermal stresses due to the mixing of hot and cooler hydrogen. Figure C.1 plots the operating conditions of both the hot upstream hydrogen and the mixed hydrogen downstream of the tee.

Table C.1—Experience with High Temperature Hydrogen Attack of 2.25Cr-1Mo Steel at Operating Conditions Below the Figure 1 Curve

			A Case B			
		Case	C			

Temperature		Hydrogen Partial Pressure (Absolute)		Time in Service Years	Description
°F	°C	psi	MPa		
675/820	357/438	1385/1570	9.54/10.82	>20	A mixing tee for the hot and cold makeup hydrogen to a hydroprocessing unit leaked near the weld to the downstream piping. SEM examination indicated decarburization and fissuring along the internal surface of the tee.
See Note	See Note	See Note	See Note		Although the leak path was not positively identified, it was concluded to be most likely due to fine, interconnected fissures. Some thermal fatigue cracking was also identified in the tee. Piping downstream of the tee was also found to have fissuring and internal decarburization to a depth of about 3.90 mils (0.1 mm) along the inside surface. The hot, upstream piping was not found to be attacked.

NOTE Average conditions are reported as first number. Maximum condition reported as second number.

[5] Communication to the API Subcommittee on Corrosion and Materials from Exxon Research and Engineering, August 1995.

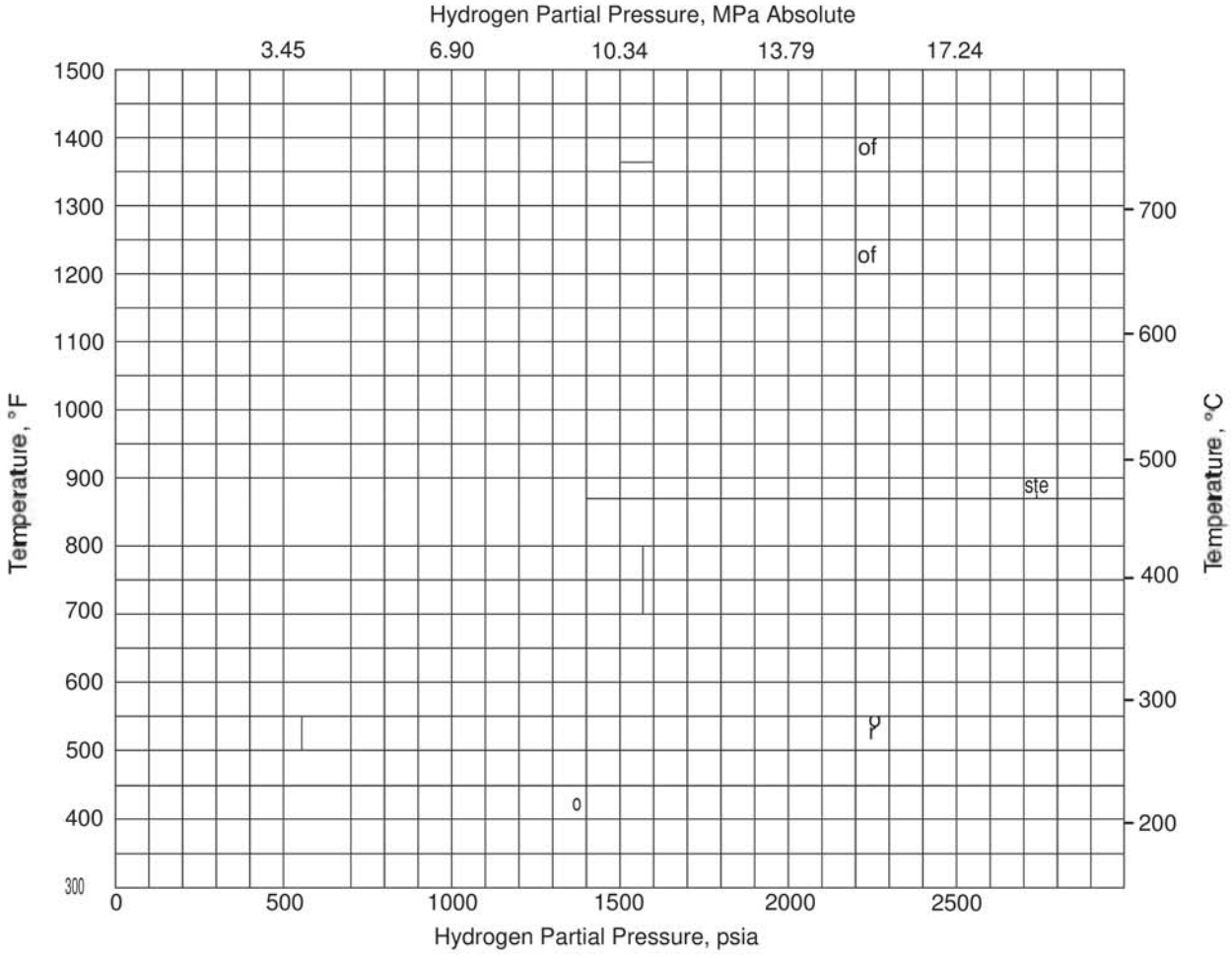

Figure C.1—Operating Conditions of 2.25Cr-1Mo Steels That Experienced High Temperature Hydrogen Attack Below the Figure 1 Curve

Annex D
(informative)

Effective Pressures of Hydrogen in Steel Covered by Clad/Overlay

The purpose of this annex is to provide a method for determining the effective hydrogen partial pressure at the clad/overlay-to-base metal interface. More details and information, such as data for solubility and diffusivity for various alloys, can be obtained in the technical basis document [39].

Very low diffusivity of hydrogen in stainless clad or s i m i l a r overlay materials used for corrosion protection results in an effective pressure of hydrogen at the clad/overlay-to-base metal interface (bond line) that is lower than that of the process stream. This effective pressure is calculated as follows:

The dimensionless number “Z” accounts for differences in the solubility/diffusivity between the cladding and base material:

$$Z = \frac{D_B X_C C_B}{D_C X_B C_C} \tag{D.1}$$

The ratio of hydrogen concentration in the operating environment to hydrogen concentration at the clad/overlay-to-base interface is given by:

$$R = \frac{1}{(1+z)} = \left(\frac{P_{H2,eff}}{P_{H2}}\right)^{\frac{1}{2}} \tag{D.2}$$

Through combination of (D.1) and (D.2), the effective hydrogen partial pressure at the clad/overlay-to-base metal interface can be determined:

$$P_{H2,eff} = P_{H2} \frac{1}{(1+z)^2} \tag{D.3}$$

Where:

D_C, D_B are the diffusivities of hydrogen in the clad/overlay and base metal, respectively. Terms are dependent on temperature and expressed in the appropriate units;

X_C, X_B are the thicknesses of the clad/overlay and base metal, respectively;

C_C, C_B are the solubilities of hydrogen in the clad/overlay and the base metal at 1 psi hydrogen partial pressure, respectively. Terms are dependent on temperature and expressed in appropriate units;

P_{H2} is the hydrogen partial pressure in the operating environment;

$P_{H2, eff}$ is the effective hydrogen partial pressure at the clad/overlay-to-base-metal interface.

Annex E
(informative)

Summary of Inspection Methods

E.1 Introduction

HTHA inspection relies on specialized techniques[1]. These techniques, procedures, and operator proficiency should be demonstrated on a broad spectrum of HTHA-damaged samples (including both damage degree and damage areas, i.e. welds and base metal). Additional details and NDE reference information will be included in the next edition of API RP 586.

E.2 Historic Inspection Approach

“Conventional” backscattered UT has been a primary technique in the past [2]. Backscattered UT includes several “sub-techniques” and are listed in this section, and these techniques for detection and characterization of HTHA are considered less effective than the new techniques listed in E3.

E.2.1 Amplitude-based

— High-frequency ultrasonic waves backscattered from within the metal are measured. HTHA can increase backscatter signal amplitude.

— Has been shown to detect HTHA fissures in base metal, away from weldments.

— Original manufacturing flaws/material inclusions can cause false positives.

E.2.2 Pattern Recognition

— High-frequency ultrasonic waves backscattered from within the metal are analyzed. HTHA causes a rise and fall in backscatter pattern.

— Has been shown to detect HTHA fissures in base metal, away from weldments.

E.2.3 Spatial Averaging

— Backscatter data are collected over an area scanned. The signal is averaged to negate grain noise.

— Has been shown to detect HTHA fissures in base metal, away from weldments.

E.2.4 Directional Dependence

— Compares backscatter signal as taken from inside diameter (ID) and outside diameter (OD) directions. HTHA-damaged materials will show a shift in indicated damage towards the exposed surface (ID).

— Has been shown to detect HTHA fissures in base metal, away from weldments.

— Orientation of damage affected by stress planes and grain structure.

— Evidence of more than one directional plane has been observed opposing this principle.

E.2.5 Frequency Dependence

— Compares backscatter of two different frequency transducers. HTHA-damaged material will show a shift and spread of backscatter in time.

— Has been shown to detect HTHA fissures in base metal, away from weldments.

E.2.6 Velocity Ratio

— Velocity ratio is a technique for indication characterization by measuring the ratio of shear wave velocity versus longitudinal wave velocity of straight beam on base metal. Based on empirical data, velocity ratio increases when there is HTHA damage in the base metal. The threshold value commonly used in the past is 0.555.

— Velocity ratio is more effective when the depth percentage of damage is relatively large, usually when it is more than 20 %. The measurement locations of shear wave and L-wave need to match very well to reduce measurement error. There are also some recent cases demonstrated that the characterization result did not match metallurgical analysis.

E.3 New Inspection Approach

While backscattered UT approach may be appropriate for complementary HTHA inspection, TOFD, PAUT (beam forming) and FMC/TFM (i.e. non-beam forming synthetic aperture PAUT techniques) are now the recommended techniques for HTHA inspection—see Table E.1a, Ultrasonic Techniques. More details about these techniques and essential variables can be found in 2019 Edition of ASME *BPV* Code Section V, Articles 1 and 4 and related Appendixes [3] and other publications focused on in-service inspections [4–13]. The use of the highest practical frequency (e.g. 7.5 MHz to 10.0 MHz) is recommended to achieve maximum detection sensitivity for the detection of microdamage. Selection of frequency of equivalent wavelength for the purpose of discriminating HTHA from metallurgical imperfections is recommended. For example, use of 10 MHz 0-degree longitudinal wave to be compared with 5 MHz transverse wave angle beam in order to determine orientation of imperfection. The use of “typical” shear wave frequency in the 3.5 MHz to 5.0 MHz range may also be included to enhance characterization of coalesced or macrocracking associated with adjacent microdamage.

E.3.1 Time of Flight Diffraction (TOFD)

— TOFD involves a pair of angled longitudinal wave probes with discrete transmitter and receiver facing towards each other on the same surface of the material being inspected.

— The transmitter emits a broad beam of energy that insonifies the area of interest. Responses from the direct path between the probes (lateral wave), reflected and diffracted energy from features within the material, and reflected energy from the far surface are detected by the receiver.

— The probe pair is scanned with a fixed separation while ultrasonic waveforms are digitized at predetermined intervals. These are used to create real-time B or D-scans typically with grayscale imaging.

E.3.2 Phased Array Ultrasonic Testing (PAUT)

— In the 2019 Edition of ASME *BPVC* Section V, *Nonmandatory Appendix E*, E-474 [14], “the UT-phased array technique is a process wherein UT data are generated by controlled incremental variation of the ultrasonic beam angle in the azimuthal or lateral direction while scanning the object under examination.”

— This process offers an advantage over processes using conventional search units with fixed beam angles, as it acquires considerably more information by covering a large range of angles (sweep).

E.3.3 Full Matrix Capture/Total Focusing Method (FMC/TFM)

— In the 2019 Edition of ASME *BPVC* Section V: Article 1, *Mandatory Appendix I, Glossary of Terms for Nondestructive Examination* [15], FMC/TFM is an industry term for an examination technique involving the combination of classic FMC data acquisition and TFM data reconstruction.

— Classic FMC: A subset of elementary FMC where the set of transmitting elements is identical to the set of receiving elements.

— Total focusing method (TFM): A method of image reconstruction where the value of each constituent datum of the image results from focused ultrasound. TFM may also be understood as a broad term encompassing a family of processing techniques for image reconstruction from FMC. It is possible that equipment of different manufacture may legitimately generate very different TFM images using the same collected data.

E.3.4 High Sensitivity Wet Fluorescent Magnetic Testing (HSWFMT)

The following is a description of the work process associated with HSWFMT. The following steps are recommended to provide and enhance the inspection sensitivity, which have been developed and optimized for HTHA damage detection, especially of non-PWHT carbon steels where cracking is most likely related to welds. Additional discussion regarding HSWFMT is provided in Table E.2.

— Surface Preparation:

  — Abrasive blasting (garnet is the preferred media) followed by smooth blending of weld cap, heat affected zone, and base material.

  — Metal removal performed using fiber discs with a final grind of 80 to 100 grit. Surface roughness should not impair particle mobility.

  — Remove 0.030 in to 0.090 in. of the wall thickness within the area to be inspected. Be mindful of the corrosion allowance.

  — Macro-etch the ground surface to be inspected. Success has been reported using three rounds of 5 % Nital in 3 minute intervals. The advantage of etching is to remove smeared metal from grinding that bridges grain boundaries. Care should be taken to avoid overetching as this may result in false positive indications.

— Application

  — Use multiple directions for both magnetic flux lines and HSWFMT solution flow. Primary direction is with the yoke positioned across the weld with the arms spaced close to concentrate magnetic flux to only 4 to 6 in. of weld length.

  — Apply magnetic fluxes using an AC yoke and HSWFMT solution for extended durations (at least 15 seconds per orientation and location) in areas to be inspected.

  — Use nonaerosol-based deployments of HSWFMT solution to allow for better particle flow control. Aerosol deployments can have similar performance, but experience has shown that indications take longer to appear.

  — Follow ASTM guidelines for fluorescent particle-to-carrier solution ratio.

  — Assure ultraviolet (UV) light source intensity and wave length is correct.

— Check AC yoke magnetic field strength frequently. Long durations of use can cause overheating and lack of magnetic flux line strength. Having two yokes will allow one to cool down while the other is in use and will ensure magnetic field strength.

— Background light limits should be checked and managed in area of inspection.

— Acute vision is essential for this inspection.

E.4 HTHA Manifestation, NDE Characterization/Categorization and Reporting

In API 579-1, draft section on assessment of HTHA damage, HTHA damage is categorized as (1) volumetric, (2) blister, (3) crack-like flaw, and (4) combination of volumetric, blister, and crack-like flaw damage [16]. An example for damage reporting is shown in Table E.3.

a) HTHA Volumetric Damage—Typically occurs in base metal and is widespread on the component. An exception is for local hot spots on high temperature components where accelerated HTHA damage may occur locally because of the high temperature. This damage is characterized by submicron intergranular voids and fissuring (see Figure E.1). Proposed NDE characterization/categorization/reporting acronym—(V).

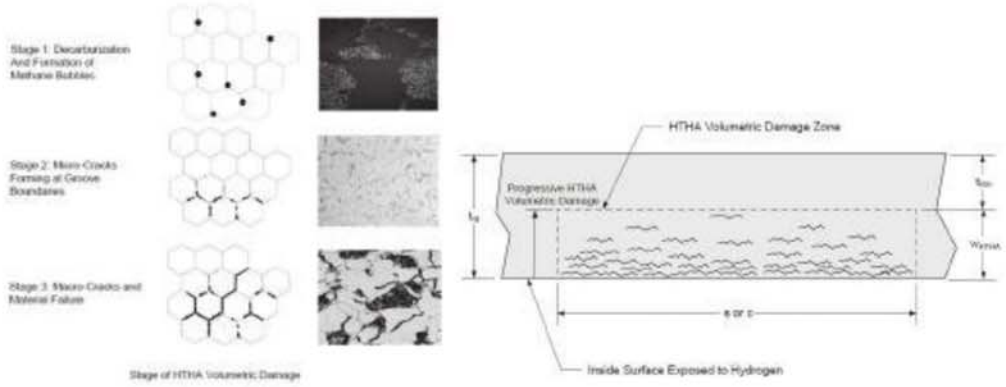

Figure E.1—HTHA Volumetric Damage Manifestation

b) HTHA Blisters—An advanced form of volumetric damage, where the methane pressure results in macro-scale fissuring in the form of blisters on the inside surface of a component (see Figure E.2). Proposed NDE characterization/categorization/reporting acronym—(B).

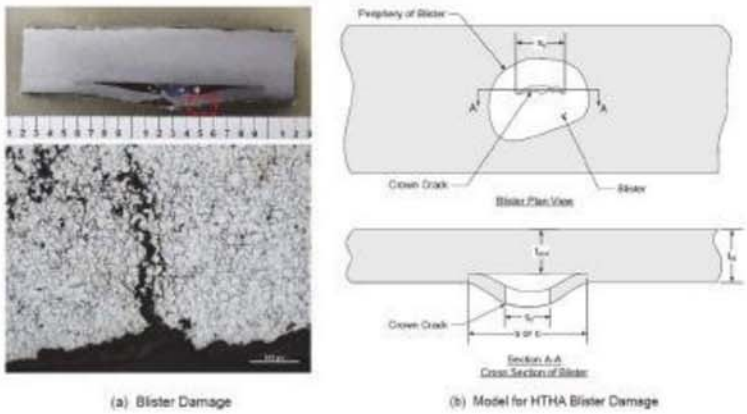

Figure E.2—HTHA Blister Damage Manifestation

c) HTHA Crack-like Flaw Damage—Typically associated with the HAZ of welds. This crack-like flaw is planar for this damage mechanism. It is characterized by cracking in the heat affected zones or fusion boundary of welds (see Figure E.3). Proposed UT characterization/categorization/reporting acronym—(C). Although this macro image highlights the crack-like flaw, less advanced HTHA damage (Stage 1 or Stage 2 damage) may be present elsewhere in the sample, as it is likely that HTHA damage extends beyond crack-like flaws.

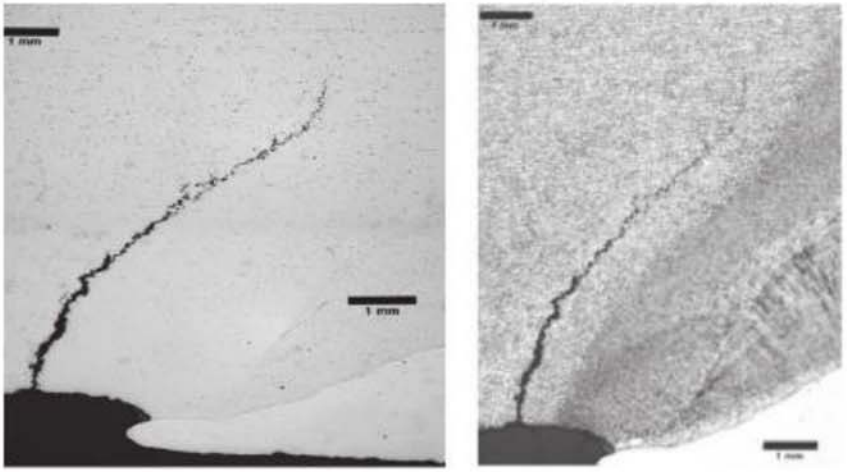

Figure E.3—HTHA Crack-like Flaw Damage Manifestation

d) HTHA Combination of Volumetric, Blister, and Crack-like Flaw Damage—Volumetric damage can occur to the base metal while crack-like flaws are occurring within the HAZ of welds (See Figure E.4). Volumetric damage that occurs ahead of the crack tip can weaken the nearby material, leading to even faster crack growth rates. Proposed UT characterization/categorization/reporting acronym—(CVBC). Note that it is also possible to have volumetric and crack-like flaws without necessarily having blisters. In advance of the cracking, it is possible to have Stage 2 damage, which is usually detectable by NDE, and Stage 1 damage, which is usually not detectable by NDE.

NOTE Metallurgical imperfections such as inclusions (I) and laminations (L) will probably be detected and may act as HTHA damage nucleation points. Welding imperfections such as lack of fusion (LOF) and lack of penetration (LOP) will probably be detected also. Additional NDE characterization is required to avoid miscategorization and false positive indications.

Figure E.4—HTHA Combination of Volumetric, Blister, and Crack-like Flaw Damage Manifestation.

Table E.1a - Ultrasonic Techniques (Recommended)

	TOFD	PAUT	FMC/TFM
Description	Diffraction and time-based. Longitudinal-longitudinal diffraction mode setup of pair transducers. B- and D-grayscale 2D image of the digitized A-scan. Higher frequencies increase capability for detection of HTHA at weldments.	Reflective and diffraction-based. Longitudinal and shear waves. Linear, 2-D matrix and annular arrays. A-, B-, C-, D-, S- scan 2D imaging. Pulse-echo scheme (using higher frequency sound) increases capability for detection of HTHA in base material and weldments/HAZ.	Reflective, diffraction and scatter-based. Longitudinal and waves. Linear and 2-D matrix arrays. A-, B-, C-, D- scan 2/3D imaging. FMC data acquisition scheme that involves the collection of all possible combinations of sources and receivers in an array, and TFM imaging scheme that involves computation of a focused image on every point of an imaged region (using high-frequency sound) to increase the capability for better detection and sizing of HTHA in base material and weldments/HAZ.
Detection Capability Effectiveness [a]	Usually Effective: Can detect HTHA in base metal, weld HAZ, and at weldments.	Usually Effective: Can detect HTHA in base metal, weld HAZ, and at weldments.	Usually effective: Can detect HTHA: in base metal, weld HAZ, and at weldments.
Sizing Effectiveness	Usually effective for length and depth (location) and height sizing. Not effective for precise depth (location), height location and sizing (width) perpendicular to the scanning direction.	Usually effective for length and width sizing when appropriate inspection setup is used.	Usually effective for length and depth (location), height and width sizing. When appropriate inspection setup is used, better effectiveness can be achieved than PAUT.
Characterization Capability	— With a combination of these techniques, proper characterization between HTHA damage and large fabrication flaws (e.g. lamination in base metal, LOP, LOF, slag, isolated porosity, and inclusion) can be effective through indication location and pattern recognition — Difficult to distinguish early-stage HTHA from inclusions/impurities. — Difficult to distinguish HTHA-induced cracking versus cracks induced with potentially other damage mechanisms from one inspection data set. — Encoded data storage makes it possible to perform more reliable monitoring of indication from multiple inspections than conventional methods. — The fundamental principles of historical characterization techniques (backscatter signal pattern recognition, frequency spectrum analysis, and velocity ratio) are still applicable to further assist in indication characterization. These techniques can be applied on data collected from new techniques (TOFD, PAUT, and TFM) to improve capability and confidence for characterization between HTHA and other damage mechanisms.		
Comments	— Higher inspection speed for a parallel scan and lower inspection speed for combined parallel and nonparallel scans. — Consideration is to be given to the blind zone created by the leading edge of the ID used. response masking low amplitude responses from adjacent flaws and/or flaws located in the shadow zone caused by the ID geometry. Similarly, inspections from the ID will create a near-surface blind zone due to the lateral wave. Supplemental techniques such as PAUT or FMC/TFM should be considered where damage within the blind zones is a concern.	Greatest effectiveness achieved in near field of the transducer (Typ. minimum of 32 elements for thickness ≤1 in. and 64 for > 1 in.). Lower inspection speed.	Greatest effectiveness achieved in near field of the transducer used and using high-density reconstruction grid. (typ. minimum of 64 elements for a typical 10 MHz transducer). Lower inspection speed.

Techniques must be developed/assessed/applied according to case-specific applications (e.g. thickness, geometry, material of construction, access, etc.)

Optimized and validated procedures to include well-tuned application specific setups for TOFD, PAUT, and FMC/TFM.

Operators should have HTHA-specific training and qualifications.

Validation or progressive qualification may be conducted using scoop or boat sampling or destructive testing.

Readers should reference API RP586 (once available) for additional detailed guidance.

Early-stage HTHA damage may not be ID surface connected.

[a] Inspection effectiveness (versus detection capability) will be covered in future effort (e.g. 586) to address 581 inspection effectiveness guidance.

Table E.1b—Historic Ultrasonic Techniques for Detection and Sizing

	Single Element A Scan Straight Beam Manual Scanning	Single Element A Scan Angle Beam Manual Scanning
Description	Use single element straight beam probe in initial scanning targeted to detect indications equivalent to the size of HTHA fissures.	Use high-frequency single element angle beam probe (flat or contour focused) in initial scanning targeted to detect indications equivalent to the size of HTHA fissures and microcracking in the heat affected zone.
Effectiveness	— Performance of manual scanning without data recording is very dependent on technician capability and condition during inspection. Therefore, the effectiveness of manual scan for detection is considered less effective than new techniques with data recording capability. — These techniques can be used as supplemental techniques in situations where initial scanning techniques with encoded data recording is not practical.	

Table E.1c—Historic Ultrasonic Techniques for Characterization

	Velocity Ratio	Attenuation	Longitudinal Spectral Analysis	Angle-beam Spectrum Analysis	Conventional Single Element A-scan Backscatter Pattern Recognition
Description	Ratio of shear and longitudinal wave velocity is measured. HTHA changes the ratio.	Dispersion of ultrasonic longitudinal wave is measured by recording drop in amplitude of multiple echoes. HTHA increases attenuation.	The first backwall signal is analyzed in terms of amplitude versus frequency. HTHA will attenuate high-frequency response more than low frequencies.	The spectrum of any suspect signal from pulse-echo inspection of weld/HAZ is compared with a reference spectrum taken in the pitch-catch mode from the base metal. HTHA causes the pulse-echo spectrum to increase amplitude with increase of frequency.	— Amplitude-based — Pattern Recognition — Spatial Averaging — Directional Dependence — Frequency Dependence
Capability	— A combination of these techniques is historically used to assist in characterizing an indication of HTHA from other flaws. — The reliability and repeatability of angle beam spectrum analysis are very dependent on subjective judgement of personnel during inspection. — Very limited data is collected for monitoring purposes, and the data collection process is time consuming.				

Table E.2—Non-ultrasonic NDT Methods for HTHA [a]

	Wet Fluorescent Magnetic Particle Testing (WFMT)	High Sensitivity Wet Fluorescent Magnetic Particle Testing (HSWFMT)	Radiographic Testing (RT)	Visual Testing (VT)	Acoustic Emission Testing (AET)
Description	Ferrous particles with fluorescent coatings suspended in liquid gather at interruptions in magnetic flux lines at the surface creating an indication. Magnetic flux should be generated by alternating current (ac). Surfaces are prepared via wire wheel or sand blasting.	See description of WFMT. Additionally, detailed surface preparations (grinding, material removal, and macro-etching) are used along with detailed application work processes. Specific work processes are discussed in more detail above.	Radiation energy is used to create an image on film or an electronic detector. Radiography is commonly used for weld quality evaluation and wall thickness measurement.	Internal VT of pressure vessels for surface blistering. White light applied parallel to the internal surface can aid in revealing blisters protruding beyond the surface plane.	Low-frequency sound waves are generated either when crack-like flaws propagate (microscopically), or during crack-tip blunting. AET for HTHA is usually executed during monitoring of thermal gradients associated with temperatures of interest so actual process-induced stresses are used. Detects and locates sound wave origins.
Detection Capability	Can detect HTHA only after cracks have formed. Cannot detect fissures or voids.	Capable of detecting randomly oriented incipient, early-stage, and late-stage HTHA damage at the inspection surface.	Can detect late-stage HTHA damage in the form of cracks. Cannot detect early-stage HTHA damage.	Surface blisters are readily apparent. HTHA damage has been detected below blistered or damaged cladding.	Capable of detecting discontinuities with high-stress concentration factors and has a higher probability of detection for late-stage HTHA damage.
Damage Sizing	Provides high confidence in indication length dimensions along with location and orientation. Cannot nondestructively determine depth.	Provides high confidence in indication width and length dimensions along with location and orientation. Cannot nondestructively determine depth.	Provides indication width and length dimensions along with location and orientation. Cannot size depth.	Can only size the perimeter of the deformed blister immediately adjacent to the surface.	AET cannot size the detected indications.
Advantages	Crack indications can be seen visually, and little interpretation is required. Large surface areas and complex geometries (including nozzles) can be inspected.	Can detect HTHA early-stage at the prepared surface. Large surface areas and complex geometries (including nozzles) can be inspected.	RT provides a visual image and can be used as a permanent record.	No special inspection tools are needed. Blister interpretation is clear.	AET is capable of inspecting several vessels and piping sections simultaneously. No practical limitation on material temperature. Often used prior to T/A to guide shutdown inspection efforts.
Limitations	Cannot detect HTHA fissures or voids. Detects only the advanced stages after surface cracks have formed. Cannot determine the depth of HTHA damage.	Only detects surface-breaking HTHA damage. Requires highly skilled technician and significant interpretation. Cannot determine the depth of HTHA damage. Only effective on the prepared surfaces.	May miss cracks, depending upon the orientation of the crack plane. RT of equipment with external coverings will reduce inspection detection sensitivity.	HTHA frequently occurs without the formation of surface blisters. Blisters, when present, are likely to be an indication of advanced HTHA. Cracking is not always visible.	Needs adequate applied stresses to create release of sound waves from the stress risers, e.g. HTHA cracks, being sought. Consequently, it is imperative that all stresses are well understood, especially during the monitoring of thermal changes, such as a planned cooldown, in order to generate a valid AET inspection.
Recommendations	Recommended for internal inspection of pressure vessels to detect surface-breaking cracks.	Recommended for internal inspection of pressure vessels to HTHA inspection to detect surface-breaking cracks and HTHA damage.	Not recommended as a primary method.	Not recommended for general HTHA detection, but may detected base metal or cladding blisters.	Recommended as a layer of protection for high risk equipment or as a global screening method. In both cases, additional more focused follow-up inspections using alternative methods are recommended.

[a] The effectiveness of all these inspection methods are dependent on highly skilled and trained NDT personnel.

Table E.3—Example for FMC/PAUT/TOFD Reporting Table

EXAMPLE: FMC or PAUT or TOFD HTHA Data Reporting Table for Hotspot # or Plate Area # or T-Junction # or Weld # of Vessel # or Piping Circuit #

(X/Y) = ...in./mm (X or Y coordinate spacing of the reference point to the nearest major structural discontinuity L_{msd}

(X/Y) = ...in./mm (X or Y coordinate spacing of the reference point to the Nearest Weld Joint) L_W

Scan/ File	t_{rd} in./mm (Wall Thickness reading)	Indication #	Isolated SIngle (Is)/ Group (G) Indication	Indication Character- ization	X-position to Reference Point (in./mm)		Y-position to Reference Point (in./mm)		Δ X, in./mm (s/longitudinal or c/circumferential extend)	Δ Y, in./mm (s/longitudinal or c/circumferential extend)	$t_{mm\ ID-}$ in./mm (Minimum measured undamaged wall thickness at ID)	$t_{mm\ OD-}$ in./mm (Minimum measured undamaged wall thickness at OD)	W_{HTHA} in./mm (Wall thickness with HTHA damage/ a-Depth per FFS which is equal to UT vertial height reading)	Comments
					From	To	From	To						

NOTE 1 Some enclature used in API 579-1, draft section on assessment of HTHA damage, is expanded for the proposed UT reporting table.

NOTE 2 No FFS Interaction rules are currently available.

L_{msd} X or Y coordinate spacing to the nearest major structural discontinuity, example nozzle.

L_W X or Y covordinate spacing to the nearest weld joint.

t_{rd} Thickness reading at the time of the FFS assessment (wall thickness).

Longitudinal extent of HTHA volumetric or other damage in a cylinder or pipe, meridional and circumferential extent of HTHA damage in a sphere (can be Δ X and Δ Y).

c Circumferential extent of HTHA volumetric or other damage, as applicable (can be Δ X and Δ Y).

Minimum measured undamaged wall thickness at ID/OD. $t_{mm\ ID\ OD-}$

W_{HTHA} Wall thickness with HTHA damage.

a Depth of the crack-like flaw per FFS assessment which is equal to the vertical measured by UT.

E.5 General Inspection Plan

The following are considerations when planning an HTHA inspection:

— Operational-based screening of equipment to estimate damage state, extent, and location with owner's mechanical integrity and operation personnel.

— PMI: Consider PMI (and alloy composition analysis) of weld filler metal on all welds and base metal to confirm uniform HTHA susceptibility.

— UT techniques should be applied from outside to the maximum extent possible. If performed from internal surface, NDE sensitivity will be reduced for near ID surface damage.

— Surface preparation is a critical parameter influencing effectiveness of all ultrasonic techniques, especially for frequencies above 5 MHz.

  — In some situations, there is incentive for the removal of weld reinforcement (cap) to enable specialized UT techniques across the weld cap.

— Inspection screening based on TOFD (to extent possible due to productivity and tolerance of flaw tilt) and complimentary FMC or PAUT techniques to confirm.

— If the inspection is based on FMC or PAUT techniques, consider complementary TOFD (to extent possible) to confirm and assist with interpretation of indications.

— Limitations: The use of highly sensitive UT techniques (e.g. high-frequency TOFD, PAUT, and FMC) are susceptible to false positive calls and challenging signal interpretation depending on circumstances. Some factors that led to these challenges include:

  — dirty steels with significant inclusions;

  — poor surface condition (scanning or non-scanning sides);

  — welds with significant fabrication flaws;

  — single-sided weld access (e.g. nozzles); and

  — NDE analysis by examiners with limited HTHA experience.

— Due to limitations of individual inspection technique, higher effectiveness is achieved using combinations of nonintrusive and intrusive technologies. Nonintrusive examples are TOFD, PAUT, and FMC. Intrusive technology examples are internal visual, HSWFMT, and metal extraction using scoop or boat sampling. The aforementioned NDT techniques are used to identify location(s) for metal extraction. Metal samples are then analyzed using metallurgical techniques for final verification.

— Effectiveness is based upon Stage 2 volumetric damage (see section on HTHA characterization within this NDE Annex) and higher for ultrasonic techniques.

— Data encoding is recommended to the extent possible since it assures full coverage, enables secondary data review and correlation among multiple techniques).

— Single element UT transducer may be useful for limited access locations when current techniques (e.g. TOFD/PAUT/FMC are not possible).

— Recommend consulting NDE subject matter expert (SME) for review and approval for all proposed HTHA inspection techniques procedures and reports.

— Operator Qualification and Training: HTHA NDT examiner should have damage mechanism-specific training using a broad spectrum of samples (damage extent and type), and sample geometries (e.g. girth welds and nozzle welds). Recommend that HTHA-specific UT method training should be a minimum of 40 hours for currently qualified and certified UT examiners. HSWFMT examiners should have similar training requirements and a minimum of 24 hours of HTHA specific training.

E.6 Cladding/WOL

The following are considerations for inspection of clad or weld overlaid equipment subject to HTHA:

— Integrity and inspection of cladding/WOL should be considered to determine HTHA susceptibly due to cladding damage.

— Cracks in cladding/WOL will decrease its effectiveness as a hydrogen barrier. A method to determine the effective hydrogen partial pressure in clad or overlaid steel is discussed in Annex D.

— Inspection of cladding/WOL itself should also be considered typically using VT, PT, and UT for cladding/WOL interface integrity.

E.7 Intrusive Inspection-narrative on When/How to Use Complementary Tools

The following are considerations when planning an intrusive inspection to look for HTHA damage:

— Planning: Review the history of the equipment item to be inspected. Search for history of indications noted, removed, repaired etc. Also, modifications made such as nozzle installation or removal, corrosion repair, crack repairs etc. Include all such items on the list for visual, PMI, and HSWFMT.

— Visual Inspection:

  — It is recommended to abrasive-blast the inside surface of the equipment being inspected.

  — White light positioned oblique to the inside surface is needed to search for blisters.

— HSWFMT may be applied to locations such as:

  — representative sample of circumferential, axial, nozzle, and attachment welds;

  — weld repaired areas;

  — those with complex geometry;

  — in areas of incorrect materials of construction;

  — high-stress areas; and

  — poor workmanship areas that indicate locations of high stress common to weld repairs and modifications.

— Metal Extraction: Prioritization of areas selected for metal extraction should include the following:

  — locations where UT examinations revealed indications;

  - — where HWFMTs revealed indications;
  - — where visual inspection detected blistering; and
  - — where PMI detected incorrect materials of construction.

- — Metal extraction locations should not be selected at random. Locations should be selected and prioritized based on evidence of anomalies.
- — Localized thin area (LTA) calculations should be conducted prior to the start of an internal inspection. Hemispherical scoop-type extractions are most favorable. Hemispherical-shaped material removal does not require weld repair if diameter and depth do not exceed LTA calculations per ASME FFS-1/API 579-1 [17].
- — Boat samples are most common for metal extractions. Weld repair is needed in most cases. Weld repair on material with HTHA damage can be difficult. Boat sample extraction configuration can be changed to hemispherical shape by grinding techniques.

E.8 Use of SEM for Metallurgical Validation of HTHA

In some cases, even when using advanced inspection techniques, it may not be possible to interpret the results without additional metallographic examination. The use of a scanning electron microscope (SEM) at magnifications greater than 1000x is recommended for the metallurgical validation process. HTHA damage (fine methane bubbles or tight cracks) near or below optical light microscopy (OLM) resolution limits has been documented in ex-service components and laboratory generated samples [18–20]. The resolution limit of OLM makes distinguishing critical differences between voids versus polishing and etching pits challenging. Both appear as dots at 1000x with OLM or very tight fissures versus heavily etched grain boundaries (both appear as dark grain boundaries at 1000x with OLM). As the NDT technologies continue to advance, it has become apparent that even early-stage HTHA damage may be detected. Use of SEM allows for more clear and definitive analysis that will help prevent false positive and false negative metallurgical validations. Metallurgical validation methods for HTHA are provided in Table E.4.

API 941 TR-A provides several examples of non-PWHT'd carbon steel equipment items in which crack-like HTHA damage has been metallurgically validated without observable decarburization [21]. Additionally, there are calculations to support this finding, which indicate the required amount of decarburization associated with crack-like HTHA formation that may be below the resolution capabilities of OLM. Thus, HTHA cracks viewed by OLM may look similiar to cracks resulting from other damage mechanisms: e.g. reheat cracking, weld metal cracking, hydrogen-induced cracking (HIC), stress corrosion cracking, and creep cracking. Guidance on HTHA manifestation and appearance is also provided in Section 4 and Annex E Section E.4 as well as the API 941 TR-A. Careful examination of the equipment operating conditions and use of SEM is critical for proper diagnosis.

Table E.4—Metallurgical Validation Methods for HTHA

	Field Metallography and Replication (FMR)	Scoop Sampling and Metallurgical Examination	Boat Sampling and Metallurgical Examination	Full Thickness Sample Removal and Metallurgical Examination
Description	Field metallography uses a microscope to directly observe the prepared surface's microstructure, and replication produces a negative film of the surface that is examined in a laboratory. In both cases, three rounds of polishing and etching are recommended for detection of HTHA damage.	Removal of metal using a spherical-shaped cutter to produce a lens of metal. Metallurgical specimens are then extracted and examined in a laboratory setting using optical microscopy, scanning electron microscopy (SEM), and limited mechanical testing.	Requires a common angle grinder. Recommend using thin wafer cut off blades to remove samples. Metallurgical specimens are then extracted and examined in a laboratory setting using OLM, SEM, and limited mechanical testing.	Hot or cold cutting of a geometric shape and remove the full wall thickness of material. Metallurgical specimens are then extracted and examined in a laboratory setting using optical microscopy, SEM, and mechanical testing.
Detection Capability	On the prepared surface, it can detect cracks, fissures, changes in microstructure, i.e. decarburization, and possibly voids. FMR is the most limited of the validation methods.	High magnification optical or electron microscopy can be used for confirmation of early-stage damage.	High magnification optical or electron microscopy can be used for confirmation of early-stage damage.	Specimens extracted from the removed material can be evaluated using high magnification optical microscopy or electron microscopy to confirm early-stage HTHA damage.
Damage Sizing	Very accurate width and length. Depth may be determined through controlled grinding and follow-up FMR. The typical area of inspection is small (less than 1 in.2) so it is commonly used for surface area damage sizing.	Can quantify the depth that a specific HTHA feature is observed, provided the damage is contained in the prepared metallurgical specimen.	Can quantify the depth that a specific HTHA feature is observed, provided the damage is contained in the prepared metallurgical specimen.	Can quantify the depth that a specific HTHA feature is observed, provided the damage is contained in the prepared metallurgical specimen.
Advantages	Can be carried out at weld metal, heat affected zone, and base metal. May confirm damage mechanism and may validate indications detected by inspection methods, e.g. UT or AET. FMR is a nondestructive method and a negative result enables the section tested to remain in service. Its biggest advantage is that results can often be found quickly while on-site.	In addition to the FMR advantages: laboratory examination results in higher sensitivity. Repair may not be necessary per results of API 579-1 FFS (Part 5) assessment.	In addition to the FMR advantages: laboratory examination results in higher sensitivity. If the boat sample divot is blend ground, repair may not be necessary per results of an API 579-1 FFS (Part 5) assessment.	Provides the most material for metallurgical examination and testing.
Limitations	Cladding must be removed. Best if 0.02 in. to 0.125 in. (0.5 mm to 3 mm) of base material is removed to reveal subsurface damage. Only surface-breaking damage on the prepared surface is detectable.	Access space is required for equipment. Specialized equipment and training is required and can be arranged to be on-site proactively or contracted once the need is identified.	Access space is required for equipment, but may be less than what is required for scoop cutting equipment. Location may require repair. Welding on HTHA damage material can be challenging. Skilled technicians are required to avoid unnecessary damage to equipment.	Location must be repaired. Welding on HTHA damage material can be challenging. Consider using a nozzle or pipe cap welded so that weld metal contacts the external surface where there is rarely any HTHA damage. Typically takes the most time to analyze the metallurgical samples.
Additional Considerations	Recommended as an informative inspection only and will be supported by the other validation methods listed in this table. May be used to trigger additional inspections.	Recommended as a high confidence follow-up inspection to the limited inspection area.	Recommended as a high confidence follow-up inspection due to limited inspection area.	Recommended as a high confidence follow-up inspection due to limited inspection area.

Evidence of decarburization at the ID surface may or may not be associated with HTHA damage and should not be used as a primary detection approach for HTHA. Surface decarburization can be associated with the manufacturing process and may be present on both inner and outer surfaces.

Regardless of metallurgical validation technique, three rounds of light etching followed by polishing are recommended to remove plastic deformation that may obscure voids and fissures.

NOTE 1

NOTE 2

NOTE 3 If cleaning between polishing steps is needed, cotton balls, or lint free wipes are recommended.

E.9 Annex E References

1) API RP 586, HTHA Inspection Techniques Section (DRAFT).

2) Wang, W.D., “Ultrasonic Detection, Characterization, and Quantification of Localized High Temperature Hydrogen Attack in Weld and Heat-affected Zone,” ASME Pressure Vessels and Piping Conference, American Society for Mechanical Engineers, New York, NY, 1999.

3) ASME Section V, Article 1 and 4, 2019 Edition.

4) https://inspectioneering.com/tag/tofd.

5) IIW V-1812-18 R1 FMC-TFM for Weld Testing (DRAFT).

6) Birring, A., M. Riethmuller. and K.Kawano, I. “Ultrasonic Techniques for Detection of HTHA, Materials Evaluation,” Vol. 63, No. 2, pp. 110-115, 2005.

7) Krynicki, J.W., K.E. Bagnoli, and J.E. McLaughlin, “Probabilistic Risk Based Approach for Performing an Onstream High Temperature Hydrogen Attack Inspection,” Paper 06580, NACE 2006.

8) Lozev, M., L. Yu, P. Mammen, T. J. Eason, J. Chew and G. Neau , “Phased Array Ultrasonic Techniques for Detection, Characterization and Sizing of High Temperature Hydrogen Attack,” 7th Biennial Inspection Summit, American Petroleum Institute, Washington, D.C., 2017.

9) Nugent, M, T. Silfies, P. Kowalski and N. Sutton, “Recent Applications of Evaluation Equipment in HTHA Service,” NACE Paper 10509, Corrosion 2018.

10) Nageswaran, C., “Maintaining the integrity of process plant susceptible to high temperature hydrogen attack. Part 1: analysis of non-destructive testing techniques,” UK HSE Research Report 1133, Prepared by TWI, 2018.

11) Krynicki, J., and J. Lilley, Advanced “Complimentary HTHA Inspection Techniques and New API 941 NDE Guidance,” 8th Biennial Inspection Summit, American Petroleum Institute, Washington, D.C., 2019.

12) Johnson, J., B. Olson, M. Swindeman, M. Carte and J. Browning, “High Temperature Hydrogen Attack Life Assessment Modeling and Inspection,” NACE Paper 13326, Corrosion 2019.

13) Neve, C.L., S. Loyan, L.L. Jeune, S. Mahaut, S. Demomte, D. Chauveau, R. Renaud, M. Tessier, N. Nauritt and A.L. Guellaut, “High Temperature Hydrogen Attack—New NDE Advanced Capabilities—Development and Feed Back,”s ASME Pressure Vessels and Piping Conference, American Society for Mechanical Engineers, New York, NY, 2019.

14) ASME *BPVC* Section V, *Nonmandatory Appendix E*, E-474.

15) ASME *BPVC* Section V: Article 1, *Mandatory Appendix I, Glossary of Terms for Nondestructive Examination,* 2019.

16) API, Recommended Practice 579-1 / ASME FFS-1, Fitness-For-Service, TBD Edition, Part 16, American Petroleum Institute, Washington, D.C., (Draft).

17) API, Recommended Practice 579-1 / ASME FFS-1, Fitness-For-Service, Third Edition, Part 1-14, American Petroleum Institute, Washington, D.C., 2015.

18) Lundin, C. and M. Bharadwaj, “Studies of High Temperature Hydrogen Related Damage in Welded Carbon Steel Components Used in Refineries,” Technical Report, The University of Tennessee, Knoxville, TN, 2015.

19) Liu, P., “Fundamental Studies of Hydrogen Attack in C-0.5Mo Steel and Weldments Applied in Petroleum and Petrochemical Industries,” Knoxville, TN: The University of Tennessee, 2001.

20) Shewmon, P. and Y. H. Xue, “Effect of High-Pressure Hydrogen on Crack Growth in Carbon Steel,” Metallurgical Transactions A, vol. 22A, no. November, pp. 2703 - 2707, 1991.

21) API, The Technical Basis Document for API RP 941, First Edition and Addendum 1, American Petroleum Institute, Washington, D.C., 2008 and 2019.

Annex F
(informative)

HTHA of Non-PWHT'd Carbon Steels

F.1 General

The purpose of this annex is to provide a brief summary of the information and experience regarding the use of welded, but not PWHT'd, carbon steels in elevated temperature and pressure hydrogen service.

In the fall of 2011 API issued an alert to inform users that there have been several reports of cracking-related issues with carbon steel piping and equipment in high temperature, high pressure hydroprocessing service at operating conditions where carbon steel was previously thought to be resistant to HTHA. Some companies no longer specify non-PWHT'd steel for new or replacement equipment used for operation up to the earlier carbon steel curve in Figure 1 because of the uncertainties regarding its performance after prolonged use. Since the year 2000, a series of unfavorable service experiences has reduced confidence in the position of the carbon steel curve for non-PWHT'd components [34].

In the Eighth Edition (2015) of this publication, a new welded carbon steel, but not PWHT'd, curve was introduced positioned at 400 °F (204 °C) from about 2200 psia (15.17 MPa) to 13,000 psia (89.63 MPa), then approximately 50 °F (28 °C) lower than the 1977 edition, from about 900 psia (6.21 MPa) to 2200 psia (15.17 MPa), then widening its separation with the non-welded or PWHT'd carbon steel curve to a maximum slightly higher than about 100 °F (56 °C) at the curve elbow to finally turn vertical at 50 psia (0.34 MPa). The past carbon steel curve will continue to be used to represent carbon steel components that are not welded or welded and PWHT'd. Plant experience has identified 12 new instances of HTHA or cracking of welded, but not PWHT'd carbon steel below the 1977 curve. The operating conditions for these instances are given in F.2 for Figure F.1 and are plotted on Figure F.1.

Prior to these recent reports, the only reported failures of carbon steel below the API RP 941, Figure 1 curve were in cases of exceptionally high stress, as discussed in 5.2 and 5.3. All of the new reports of HTHA involve carbon steel equipment that was not PWHT'd after welding during fabrication. Past research summarized in API TR 941, *The Technical Basis Document for API RP 941*, states that non-PWHT'd welds not only retain high residual welding stresses, but also have lower carbide stability in the weld HAZ that further increases HTHA susceptibility.

Existing equipment with non-PWHT'd welded carbon steel that is operated above the new non-PWHT'd welded carbon steel curve in Figure 1 should be evaluated in regards to HTHA risk. Owners/operators may choose to replace such equipment or prioritize such equipment operating above the new curve for inspection. Plant experience suggests that important variables to consider in prioritizing equipment for inspection include severity of operating condition (hydrogen partial pressure and temperature), thermal history of the steel during fabrication, stress, cold work, and cladding composition and thickness, when present.

Owners/operators should add a safety factor even to the new Figure F.1 curve, because operations just below the curve may still be at-risk due to issues such as discrepancies in temperature measurement, fouling of heat transfer surfaces, and temperature excursions.

F.2 References and Comments for Figure F.1

F.2.1 Figure F.1 References

34) J. McLaughlin, J. Krynicki, and T. Bruno, "Cracking of Non-PWHT'd Carbon Steel Operating at Conditions Immediately Below the Nelson Curve," *Proceedings of 2010 ASME Pressure Vessels and Piping Conference, July 2010, Bellevue Washington*, PVP2010-25455.

35) Eight separate points, 35a through 35h. Valero Energy Corporation, private communication to API Subcommittee on Corrosion, 2012.

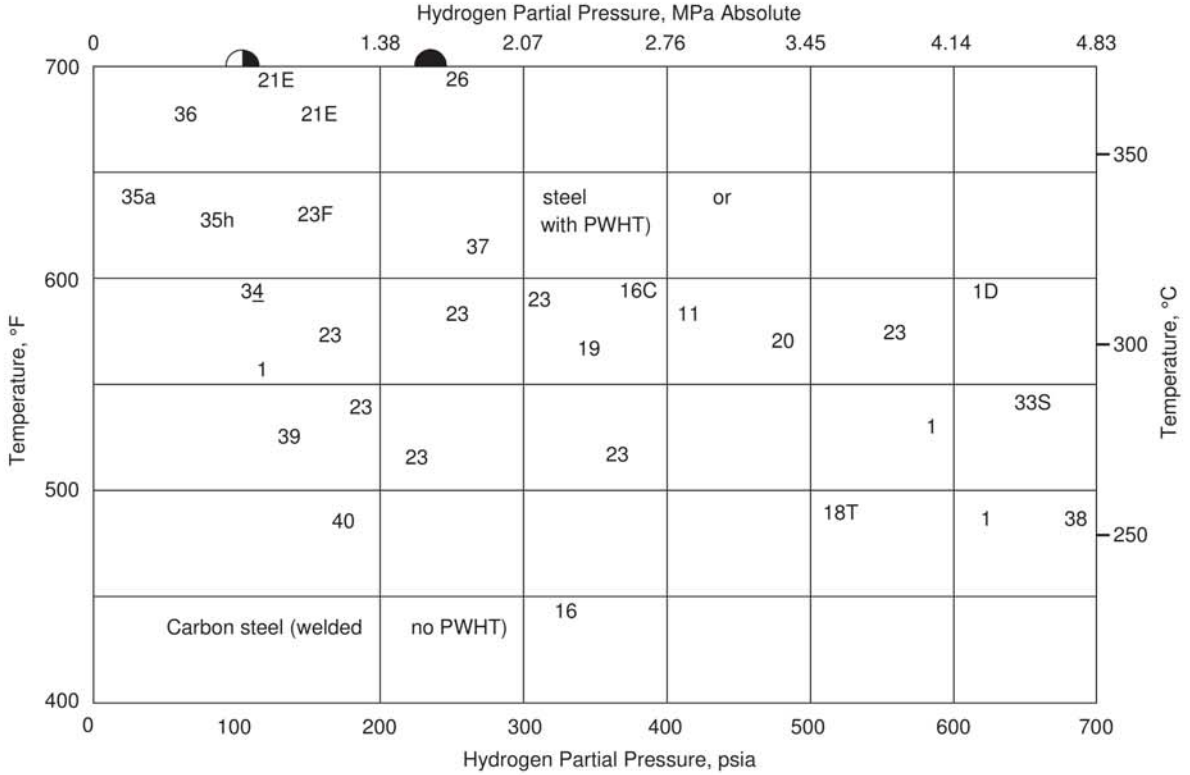

NOTE This Figure is adapted from Figure 1, Eighth Edition (2016) of this publication. Numbered and lettered references for point in this figure refer to data listed in 3.5 and F.2.

Figure F.1—Operating Conditions for Carbon Steel (Welded with No PWHT) That Experienced HTHA Below the 1977 Carbon Steel Figure 1 Curve

36) Phillips 66 Company, private communication to API Subcommittee on Corrosion, 2012.

37) Phillips 66 Company, private communication to API Subcommittee on Corrosion, 2012.

38) Total Refining and Marketing, private communication to API Subcommittee, 2011.

39) Marathon Petroleum Co., private communication to API Subcommittee, 2014.

40) Marathon Petroleum Co., private communication to API Subcommittee, 2014.

F.2.2 Figure F.1 Comments

V) Point 34. After 30+ years, non-PWHT'd carbon steel reactor, vessels, and associated piping in light distillate hydrotreating service cracked from HTHA. Operating at roughly 580 °F and at 125 psia.

W) Points 35a and 35h. These 2 points on the plot represent the range of 8 different failures. After 4.5 to 8 years, 7 different non-PWHT'd carbon steel flanges cracked in the HAZs on the flange side of a flange-to-pipe welds in gasoline hydrotreating service. One cracked on the pipe side of the pipe-to-flange weld. Operating at 645 °F (340 °C) and 57 psia to 94 psia (0.39 MPa to 0.65 MPa) hydrogen partial pressure.

X) Point 37. After 14 years, non-PWHT'd SA-105 carbon steel flange cracked in the HAZ on the flange side of a flange to pipe weld. Operating at roughly 600 °F and at 280 psia.

Y) Point 36. After 6 years, multiple non-PWHT'd carbon steel flanges cracked in the HAZs on the flange side of flange to pipe welds in a gasoline desulfurization unit. Operating at roughly 670 °F and at 85 psia.

Z) Point 38. After 29 years, non-PWHT'd carbon steel exchanger shell in HDS service cracked. Operating at roughly 500 °F and at 670 psia.

A.1) Point 39. After 10 years, inspection found cracks in non-PWHT'd carbon steel exchanger shell in light hydrotreater service. Operating at roughly 540 °F and at 130 psia.

B.1) Point 40. After 30+ years, inspection found cracks in non-PWHT'd carbon steel exchanger shell in light hydrotreater service. Operating at roughly 490 °F and at 195 psia.

F.3 Annex F References

J. McLaughlin, J. Krynicki, and T. Bruno, "Cracking of Non-PWHT'd Carbon Steel Operating at Conditions Immediately Below the Nelson Curve," *Proceedings of 2010 ASME Pressure Vessels and Piping Conference, July 2010, Bellevue Washington*, PVP2010-25455.

Chemical Safety Board draft report titled "Draft Report 2010-08-I-WA, Tesoro Anacortes Refinery."

D. Miller, API letter to The Honorable Rafael Moure-Eraso of the CSB, dated March 14, 2014, titled "Draft Report 2010-08-I-WA, Tesoro Anacortes Refinery."

Annex G
(informative)

Methodology for Calculating Hydrogen Partial Pressure in Liquid-filled Piping

G.1 General

This annex addresses the issue of calculating the hydrogen partial pressure to be applied to Figure 1 for liquid only or liquid-filled systems, where the liquid contains dissolved hydrogen, but there is no separate vapor phase present, both with and without downstream increases in total pressure. The RP is to use the hydrogen partial pressure of the vapor that was last in equilibrium with the liquid in question, or the calculated hydrogen partial pressure that would be in equilibrium with the liquid at its operating temperature and pressure. Prior to the Eighth Edition of this RP, it did not address the issue of a liquid containing dissolved hydrogen that is pumped to a pressure above its bubble point. For such a liquid, there is no “co-existing” vapor to examine for hydrogen partial pressure; however, the dissolved hydrogen in the liquid can lead to HTHA.

Examples of liquid-filled lines containing hydrogen include hydroprocessing unit separator liquid lines (upstream of pressure let-down valves), some hydroprocessing unit feed lines and equipment (when hydrogen is injected as a soak gas and then is completely absorbed by the liquid as the temperature increases), gasoline desulfurization units with pumping of the reactor bottoms streams, some biofuel units, some coal liquefaction units, and some gasification units.

Operating companies observed piping failure in pressurized liquid services containing dissolved hydrogen where the piping was thought to be in compliance with this RP. This annex contains five proposed methods to enable engineers to use this RP for pressurized liquid services.

The five methods are as follows.

— *Conventional Thermodynamics*

1) The partial pressure of dissolved gaseous species is generally defined as the partial pressure of the dissolved species (in vapor) in equilibrium with the liquid at the same temperature (i.e. the partial pressure downstream of the pumps is assumed to be very close to the partial pressure upstream). Process modeling experts report that this should be very close to the actual value (within 5 %).

2) This is consistent with the previous API 941 guidance and is appropriate for liquid lines from vessels down to pumps.

— *Total Pressure Method*

1) Start with the pressurized liquid and reduce the pressure to the bubble point. Calculate the hydrogen mole fraction of the incipient vapor.

2) Determine the pressurized liquid effective ppH_2 by multiplying that mole fraction by the total (absolute) pressure of the pressurized liquid.

For liquids that are pumped from bubble point to some higher pressure, the practitioner can simply start with the known equilibrium vapor phase properties, prior to pumping.

The other possible calculation methods are as follows:

— Pure Hydrogen Equivalency Method,

— Fugacity Correction Method, and

— Composition Variation and Compensation Method.

These tend to give results within 5 % of the Conventional Thermodynamics Method.

— *Pure Hydrogen Equivalency Method*

1) Using an appropriate thermodynamic method, calculate the fugacity of hydrogen in the liquid phase. Actual temperature and pressure should be used.

2) Find the pressure of a pure hydrogen stream (at the same temperature) such that the hydrogen fugacity is the same. The resulting pure hydrogen pressure (absolute) is the effective ppH_2 of the stream in question.

The hydrogen equivalency method finds the pure hydrogen pressure that would have the same HTHA propensity as the subject pressurized stream with dissolved hydrogen. Since the Nelson curves are drawn with ppH_2 as the independent variable, this method will often result in a higher HTHA propensity (effective ppH_2) than the simple ppH_2 would indicate.

— *Fugacity Correction Method*

1) Start with the pressurized liquid and reduce the pressure to the bubble point. Calculate the hydrogen fugacity (it will be the same for both phases) and ppH_2 for the equilibrium vapor phase.

2) Calculate the hydrogen fugacity in the liquid after pressurization.

3) The ratio of the hydrogen fugacity at higher pressure to the hydrogen fugacity at the lower pressure equilibrium is the fugacity correction factor.

4) To find the effective ppH_2 for the high pressure liquid, multiply the equilibrium vapor phase ppH_2 by the correction factor.

For liquids that are pumped from bubble point to some higher pressure, the practitioner can simply start with the known vapor phase ppH_2 prior to pumping and apply the correction factor to account for the pressure increase.

This method rigorously corrects for the increase in HTHA propensity, while maintaining consistency with the data in this RP.

— *Composition Variation + Compensation Method*

1) Again start with a pressurized liquid and appropriate thermodynamic model.

2) Hold state and compositional variables constant, then add hydrogen until the sub-cooled liquid reaches the bubble point.

3) The pseudo-saturation H_2 partial pressure is determined.

4) This pseudo-saturation value is multiplied by the ratio of actual H_2 in the sub-cooled liquid to compensate for the H_2 addition, thus arriving at the sought after effective H_2 partial pressure.

G.2 Example 1 Showing the Total Pressure Method, the H_2 Equivalency Method, and the Fugacity Correction Method

Figure G.1 below shows a typical example analysis. A narrow boiling range heavy cat naphtha (HCN) is drawn from a high pressure separator operating at 650 °F, 295 psig, and 124 psia ppH_2. The hydrocarbon liquid has a boiling range

of 384 °F to 443 °F (by ASTM D86 Method for Distillation of Petroleum Products). The pump increases the pressure by 100 psi.

Table G.1 shows the effective hydrogen partial pressures for the streams before and after the pump (A and B) using the three methods.

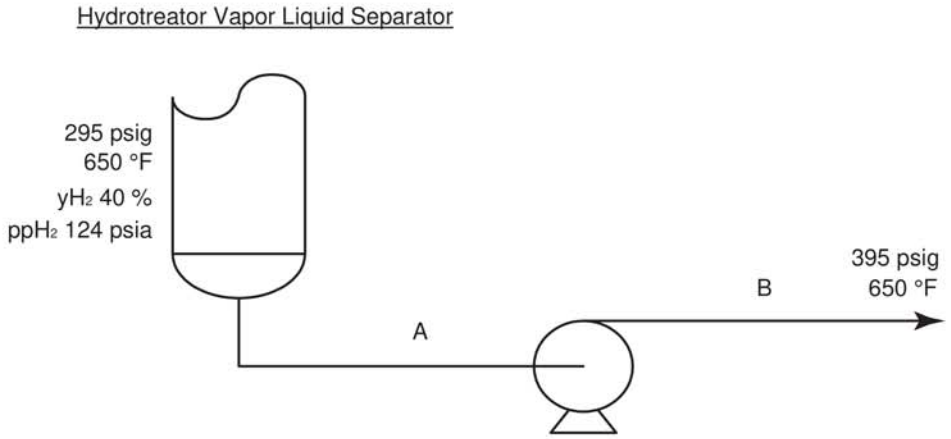

Figure G.1—Sketch for Example 1

Table G.1—Effective Hydrogen Partial Pressures

All values are psia

Calculation Method	Effective ppH2 at A	Effective ppH2 at B
Previous edition of API RP 941 (Conventional Thermodynamics)	124	164
Total Pressure Method	124	164
Pure H2 Equivalency	153 (Note)	162
Fugacity Correction Method (factor = 1.0595)	124	131
NOTE With the Pure Hydrogen Equivalency Method, the dissolved hydrogen before the pump has the same fugacity (chemical potential and activity) as pure hydrogen at 153 psia (for 650 °F). This is a higher value than the 124 psia ppH2 as calculated using API RP 941.		

	Thermodynamic Definition	Total Pressure	Hydrogen Equivalency	Fugacity Correction Factor	Composition Variation + Compensation
H2 pp	633.6	779.8	646.1	620.1	630.1
% difference	0.0	23.1	2.0	2.1	0.6
Effective H2 pp at this location	A	B	B	B	B

G.3 Example 2 Showing the Methods in Example 1 with the Composition Variation + Compensation Method

Figure 2 is for use with the following example.

— Simulate a separator with a H2-Cetane (n-C16) liquid packed line at 550 °F, 650 psia. The hydrogen molar percentage at the separator is 97.5 % with a H2 pp of 633.6 psia. The new conditions at point B are 550 °F and 800 psia.

— H2-Cetane system is an idealization of a diesel hydrotreater.

— Bottoms of separator taken through a pump with a pressure differential of 150 psi.

— The H2 partial pressure determined at the discharge using the various methods described above is presented in Table G.2.

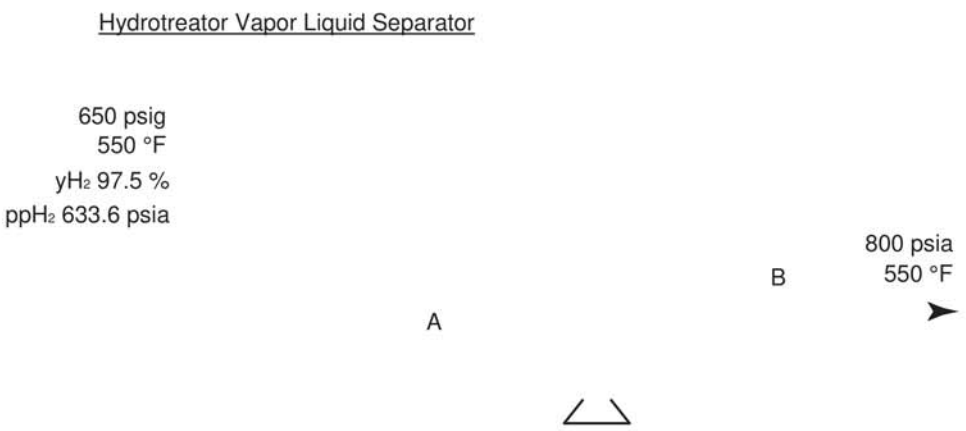

Figure G.2—Sketch for Example 2

Table G.2—Effective Hydrogen Partial Pressures with the Composition Variation + Compensation Method

Calculation Method	Effective ppH2 at A	Effective ppH2 at B
Previous edition of API RP 941 (Conventional Thermodynamics)	124	164
Total Pressure Method	124	164
Pure H2 Equivalency	153 (Note)	162
Fugacity Correction Method (factor = 1.0595)	124	131

NOTE With the Pure Hydrogen Equivalency Method, the dissolved hydrogen before the pump has the same fugacity (chemical potential) as pure hydrogen at 153 psia (for 650 °F). This is a higher value than the 124 psia ppH2 as calculated using API RP 941.

	Thermodynamic Definition	Total Pressure	Hydrogen Equivalency	Fugacity Correction Factor	Composition Variation + Compensation
H2 pp	633.6	779.8	646.1	620.1	630.1
% difference	0.0	23.1	2.0	2.1	0.6
Effective H2 pp at this location	A	B	B	B	B

G.4 Annex G References

P66 Technical Memorandum titled "Estimating Hydrogen Attack Potential for Pressurized Liquids Containing Dissolved Hydrogen," from Mitch Loescher, dated Sept. 1, 2011

"Methods for Approximating H2 Partial Pressure in Subcooled Liquids," presented at NACE CTW, Sept. 17, 2012, by Cathy Shargay, Alex Cuevas, Paul Mathias, and Garry Jacobs of Fluor.

Annex H
(informative)

Internal Company Data Collection

Request for New Information

The API Subcommittee on Corrosion and Materials collects data on the alloys shown in all figures or similar alloys that may come into use. Revisions to the curves will be published as the need arises.

For the existing curves, data are desired for instances of HTHA damage that occur above or below the curve for the steel involved; data are also desired for successful experience in the area above the curve for the steel involved. For chromium-molybdenum steels not included on the existing figures, data for successes and HTHA damage in any meaningful area are desired.

The following datasheet is provided for the reader's convenience in submitting new data. Available data should be furnished by inserting information in the spaces provided and checking the appropriate answer where a selection is indicated. Any additional information should be attached.

While both hydrogen partial pressure and temperature are important, particular attention should be given to obtaining the best estimate of accurate metal temperature. One method of obtaining more accurate data for a specific area is to attach a skin thermocouple to the area that previously exhibited high temperature hydrogen damage.

The completed form should be returned to the following address:

American Petroleum Institute
API Standards Department
200 Massachusetts Avenue, NW
Suite 1100
Washington, DC 20001

Datasheet for Reporting High Temperature Hydrogen Attack (HTHA) of Carbon and Low-alloy Steels

Date _____ File No. _____

By _____

(Name, Company, Address)

1. (a) ASTM specification (or equivalent) for the steel: _____

   (b) Design Code_____ _____

2. (a) Composition of steel (wt%) Fe _____ Cr_____ Mo _____ V _____ Ni _____ P_____ Sn _____

   Ti _____ Nb _____ C _____ Si _____ Mn_____ S_____ As _____

   (b) Steel protection: None _____ Weld overlay material _____ Sb _____

   Cladding material _____ Other _____

   (c) Thickness Base metals _____ Weld overlay or cladding (if any) _____

3. Heat treatment: Postweld heat treatment Yes _____ No _____ Temperature/Time _____ °F/hr

   Normalized and tempered Yes _____ No _____ Tempering Temperature _____ °F

   Quenched and tempered Yes _____ No _____ Tempering Temperature _____ °F

   Other _____

4. Mechanical properties (prior to exposure): Yield strength (actual) _____ psi

   Ultimate strength (actual) _____ psi

5. Temperature: Process: Average _____ °F Maximum _____ °F

   Metal: Average _____ °F Maximum _____ °F

6. Hydrogen partial pressure: _____ psia (Describe method) Hydrogen purity _____ %

7. Calculated operating stress: _____ psi

8. Microhardness: For a failure, at or near crack: _____

   For successes: Weld: _____ Base material _____

   Heat-affected zone: _____

9. Days in service: Total _____ At maximum temperature _____

10. Damage Appearance

Surface decarburization	Yes _____	No _____	Surface cracking	Yes _____	No _____
Internal decarburization	Yes _____	No _____	Internal fissuring	Yes _____	No _____
Blisters	Yes _____	No _____	Isolated Blisters	Yes _____	No _____
Voids	Yes _____	No _____			

11. Location of failure (include photograph):

Weld metal	Yes_____	No_____	Heat-affected zone	Yes_____	No_____
Base material	Yes_____	No_____			

Other _____

12. The type of process unit involved _____

13. Type of equipment (piping, vessels, heat exchanger, etc.) _____

14. Submit a photomicrograph showing typical failure and grain structure. Include 100X and 500X photomicrographs, plus any other appropriate magnifications. Attach any reports, if available. Please note any unusual circumstances.

Bibliography

In addition, this publication draws upon the work referenced in the following publications.

[1] G.A. Nelson, “Hydrogenation Plant Steels,” *1949 Proceedings*, Vol. 29M, API, Washington, DC, pp. 163–174.

[2] W.A. Pennington, *Transactions of the American Society for Metals*, Vol. 37, 1946.

[3] E.E. Fletcher and A.R. Elsea, “Defense Metals Information Center Report 202,” Battelle Memorial Institute, Columbus, Ohio, 1964.

[4] API Publication 945, *A Study of the Effects of High-temperature, High-pressure Hydrogen on Low-alloy Steels*, API, Washington, DC, 1975 (out of print).

[5] F.K. Naumann, “Influence of Alloy Additions to Steel Upon Resistance to Hydrogen Under High Pressure,” Technische Mitteilungen Krupp, Vol. 1, No. 12, pp. 223–234, 1938.

[6] API Publication 940, *Steel Deterioration in Hydrogen*, API, Washington, DC, 1967 (out of print).

[7] R.D. Merrick and C.J. Maguire, “Methane Blistering of Equipment in High Temperature Service,” Paper No. 30 presented at the Annual Meeting of the National Association of Corrosion Engineers, March 1979.

[8] I. Class, “Present State of Knowledge in Respect to the Properties of Steels Resistant to Hydrogen Under Pressure,” *Stahl and Eisen*, Vol. 80, pp. 1117–1135, Aug. 18, 1960.

[9] R.P. Jewett, “Effect of Gaseous Hydrogen on the Mechanical Properties of Metals Used in the Petroleum Industry,” *1979 Proceedings, Refining Department*, Vol. 58, API, Washington, DC, pp. 151–160.

[10] T. Nomura, K. Murayama, and M. Matsushita, “Sample Test Results of All Liquid Phase Hydrogen Attack,” Japan Energy Corporation, presented to the API Task Group on Hydrogen Deterioration of Steels, May 1994.

[11] F.H. Vitovec, “The Growth Rate of Fissures During Hydrogen Attack of Steels,” *1964 Proceedings*, Vol. 44, API, Washington, DC, pp. 179–188.

[12] G. Sundararajan and P. Shewmon, “The Kinetics of Hydrogen Attack of Steels,” *Metallurgical Transactions A*, Vol. 12, pp. 1761–1765, 1981.

[13] B.L. Chao, G.R. Odette, and G.E. Lucas, “Kinetics and Mechanisms of Hydrogen Attack in 2.25Cr-1Mo Steel,” ORNL/Sub/82-22276/01, August 1988.

[14] G.A. Nelson, “Operating Limits and Incubation Times for Steels in Hydrogen Service,” *1965 Proceedings*, Vol. 45, API, Washington, DC, pp. 190–195.

[15] R.D. Merrick and A.R. Ciuffreda, “Hydrogen Attack of Carbon-0.5Molybdenum Steels,” *1982 Proceedings, Refining Department*, Vol. 61, API, Washington, DC, pp. 101–114.

[16] M.G. Maggard, “Detecting Internal Hydrogen Attack,” *Oil and Gas Journal*, March 10, 1980, pp. 90–94.

[17] K. Ishii, K. Maeda, R. Chiba, and K. Ohnishi, “Intergranular Cracking of C-0.5Mo Steel in a Hydrogen Environment at Elevated Temperatures and Pressures,” *1984 Proceedings, Refining Department*, Vol. 63, API, Washington, DC, pp. 55–64.

[18] R. Chiba, K. Ohnishi, K. Ishii, and K. Maeda, "Effect of Heat Treatment on the Resistance of C-0.5Mo Steel Base Metal and Its Welds to Hydrogen Attack," *1985 Proceedings, Refining Department*, Vol. 64, API, Washington, DC, pp. 57–74.

[19] M. Prager, "Hydrogen Attack Susceptibility of Chrome-Moly Steels and Weldments," PVP-Vol. 239/MPC-Vol. 33, *Serviceability of Petroleum, Process, and Power Equipment*, ASME, New York, 1992.

[20] E.A. Sticha, "Tubular Stress-Rupture Testing of Chromium-Molybdenum Steels with High-Pressure Hydrogen," *Journal of Basic Engineering*, Vol. 91, ASME, New York, pp. 590–592, December 1969.

[21] E.B. Norris and E.A. Sticha, "Effect of Hydrogen on the Stress-Rupture Strength of 2-1/4Cr-1Mo Steel," *Metal Properties for the Petroleum and Chemical Industries* (ASME G00103/MPC-2), ASME, New York, pp. 590–592, 1976.

[22] A.R. Ciuffreda, N.B. Heckler, and E.V. Norris, "Stress Rupture Behavior of Cr-Mo Steels in a High Pressure Hydrogen Environment," ASME H00227/MPC-18, ASME, New York, 1982.

[23] K.R. Lewis, Shell Global Solutions—International, NACE Refin*Cor, 98C5.14.

[24] Exxon Research & Engineering, private communication to API Subcommittee on Corrosion and Materials, August 1995.

[25] D.C. Cherrington and A.R. Ciuffreda, "Design of Piping Systems for Hydrogen Service," *1967 Proceedings, Division of Refining*, Vol. 47, API, New York, pp. 237–252.

[26] T. Ishiguro, K. Kimura, T. Hatakeyama, T. Tahara, and K. Kawano, "Effect of Metallurgical Factors on Hydrogen Attack Resistance in C-0.5Mo Steel," presented at the Second International Conference on Interaction of Steels with Hydrogen in Petroleum Industry Pressure Vessel and Pipeline Service, Materials Properties Council, Vienna, Austria, Oct. 19–21, 1994.

[27] M.H. Armbruster, "The Solubility of Hydrogen at Low Pressure in Iron, Nickel, and Certain Steels at 400 to 600C," *Journal of the American Chemical Society*, Vol. 65, p. 1043, 1943.

[28] W. Geller and T. Sun, "Influence of Alloy Additions on Hydrogen Diffusion in Iron and Contribution to the System Iron-Hydrogen," *Archiv für das Eisenhüttenwesen*, Vol. 21, pp. 423–430, 1950.

[29] T.P. Groeneveld and A.R. Elsea, "Permeation of Hydrogen at Elevated Temperatures and Pressures Through Stainless Steel-Overlayed 2.25Cr-1Mo Steel," *Proceedings of API, Division of Refining*, Vol. 56 (Midyear Meeting, May 9–12, 1977, Chicago, IL), pp. 7–16. API, Washington, DC, 1977.

[30] "Report on the Effect of Stainless Steel Weld Overlay or Cladding on Hydrogen Attack of Underlying Steel," Materials Properties Council, New York, September 1984.

[31] Archakov and Grebeshkova, Reference 105 in *Welding Research Council Bulletin 275*, "The Use of Quenched and Tempered 2.25 Cr-1Mo Steel for Thick Wall Reactor Vessels, etc.," W.E. Erwin and J.C. Kerr, February 1982.

[32] Exxon Report: "Hydrogen Attack of Gofiner Reactor Inlet Nozzle," 1988.

[33] G.R. Prescott, "History and Basis of Prediction of Hydrogen Attack of C-0.5Mo Steel," a state-of-the-art review presented at Second International Conference on Interaction of Steels with Hydrogen in Petroleum Industry Pressure Vessel and Pipeline Service, Materials Properties Council, Vienna, Austria, Oct. 19–21,1994.

[34] W.D. Wang, “Inspection of Refinery Vessels For Hydrogen Attack Using Ultrasonic Techniques,” *Review of Progress in Quantitative Nondestructive Evaluation*, Vol. 12, edited by D.O. Thompson and D.E. Chement, Plenum Press, New York.

[35] W.D. Wang, “Ultrasonic Detection of High Temperature Hydrogen Attack,” United States Patent #5,404754, issued April 11, 1995.

[36] W.D. Wang, “Ultrasonic Detection, Characterization, and Quantification of Localized High Temperature Hydrogen Attack In Weld Heat Affected Zone,” *In Service Experience In Fossil and Nuclear Power Plants*, PVP-Vol. 392, edited by J. Pan, ASME, New York, 1999, pp. 291–298.

[37] W.D. Wang, “Ultrasonic Techniques for Inspection of Weld and Heat-Affected Zone for Localized High Temperature Hydrogen Attack,” United States Patent #6,125,704, issued Oct. 3, 2000.

[38] R. Bruscato, “Temper Embrittlement and Creep Embrittlement of 2.25Cr-1Mo Shielded Metal-Arc Weld Deposits,” *Welding Journal*, Vol. 49, Res. Suppl., pp 148–156, April 1970.

[39] API TR 941, *The Technical Basis Document for API RP 941*, 2008.

[40] J. McLaughlin, J. Krynicki, and T. Bruno, “Cracking of Non-PWHT’d Carbon Steel Operating at Conditions Immediately Below the Nelson Curve,” *Proceedings of 2010 ASME Pressure Vessels and Piping Conference, July 2010, Bellevue, Washington*, PVP2010-25455.

[41] T. Kushida, NACE Corrosion 1994 Paper No. 67 (Fig. 10).

[42] ASME *Boiler and Pressure Vessel Code* (*BPVC*), *Section II: Materials; Part A: Ferrous Material Specifications*

[43] ASME *Boiler and Pressure Vessel Code* (*BPVC*), *Section II: Materials; Part D: Properties*

[44] ASME *Boiler and Pressure Vessel Code* (*BPVC*), *Section III: Rules for Construction of Nuclear Power Plant Components*

[45] ASME *Boiler and Pressure Vessel Code* (*BPVC*), *Section VIII; Division 3: Alternate Rules for Construction of High Pressure Vessels*

[46] ASME/ANSI *Code for Pressure Piping* B31.12, *Hydrogen Piping and Pipelines*

[47] ASTM D86, *Standard Test Method for Distillation of Petroleum Products at Atmospheric Pressure*

[48] ASTM A204, *Standard Specification for Pressure Vessel Plates, Alloy Steel, Molybdenum*

[49] SAE AMS5046D, *Carbon Steel, Sheet, Strip, and Plate* (SAE 1020 and 1025), *Annealed*

200 Massachusetts Avenue, NW
Suite 1100
Washington, DC 20001-5571
USA

202-682-8000

Additional copies are available online at www.api.org/pubs

Phone Orders: 1-800-854-7179 (Toll-free in the U.S. and Canada)
303-397-7956 (Local and International)
Fax Orders: 303-397-2740

Information about API publications, programs and services is available on the web at www.api.org.

Product No. C94108